

ARMY RESEARCH LABORATORY



Investigation of Surface Intergranular Attack and Its Effects on the Fatigue Properties of AM355 Stainless Steel

Scott Grendahl
Victor Champagne

ARL-TR-1238

November 1996

DTIC QUALITY INSPECTED 4

19961223 098

NOTICES

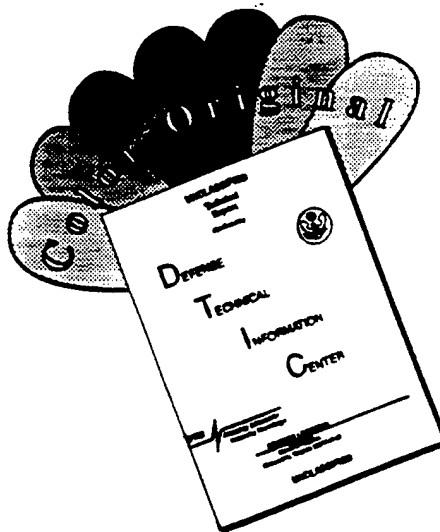
Destroy this report when it is no longer needed. DO NOT return it to the originator.

Additional copies of this report may be obtained from the National Technical Information Service, U.S. Department of Commerce, 5285 Port Royal Road, Springfield, VA 22161.

The findings of this report are not to be construed as an official Department of the Army position, unless so designated by other authorized documents.

The use of trade names or manufacturers' names in this report does not constitute indorsement of any commercial product.

DISCLAIMER NOTICE



THIS DOCUMENT IS BEST QUALITY AVAILABLE. THE COPY FURNISHED TO DTIC CONTAINED A SIGNIFICANT NUMBER OF COLOR PAGES WHICH DO NOT REPRODUCE LEGIBLY ON BLACK AND WHITE MICROFICHE.

REPORT DOCUMENTATION PAGE			Form Approved OMB No. 0704-0188	
Public reporting burden for this collection of information is estimated to average 1 hour per response, including the time for reviewing instructions, searching existing data sources, gathering and maintaining the data needed, and completing and reviewing the collection of information. Send comments regarding this burden estimate or any other aspect of this collection of information, including suggestions for reducing this burden, to Washington Headquarters Services, Directorate for Information Operations and Reports, 1215 Jefferson Davis Highway, Suite 1204, Arlington, VA 22202-4302, and to the Office of Management and Budget, Paperwork Reduction Project(0704-0188), Washington, DC 20503.				
1. AGENCY USE ONLY (Leave blank)		2. REPORT DATE November 1996		3. REPORT TYPE AND DATES COVERED Final, Dec 95 - Feb 96
4. TITLE AND SUBTITLE Investigation of Surface Intergranular Attack and Its Effects on the Fatigue Properties of AM355 Stainless Steel			5. FUNDING NUMBERS PR: 1L162618AH80	
6. AUTHOR(S) Scott Grendahl and Victor Champagne				
7. PERFORMING ORGANIZATION NAME(S) AND ADDRESS(ES) U.S. Army Research Laboratory ATTN: AMSRL-MA-CB Aberdeen Proving Ground, MD 21005-5069			8. PERFORMING ORGANIZATION REPORT NUMBER ARL-TR-1238	
9. SPONSORING/MONITORING AGENCY NAMES(S) AND ADDRESS(ES) U.S. Army Aviation and Troop Command 4300 Goodfellow Blvd. St. Louis, MO 63120-1798			10. SPONSORING/MONITORING AGENCY REPORT NUMBER	
11. SUPPLEMENTARY NOTES				
12a. DISTRIBUTION/AVAILABILITY STATEMENT Approved for public release; distribution is unlimited.			12b. DISTRIBUTION CODE	
13. ABSTRACT (Maximum 200 words) A critical flight safety component fabricated from AM355, a semiaustenitic precipitation hardenable stainless steel, from an Army attack helicopter failed catastrophically in service. The U.S. Army Research Laboratory (ARL) performed an in-depth metallurgical analysis of the broken component, which revealed that the premature failure was attributable to fatigue. Further analysis of material taken from various stages of processing revealed an intergranular surface attack that ARL determined to be caused by acid pickling during primary processing. ARL hypothesized that the surface intergranular attack may have led to premature crack initiation due to the breakdown of the protective passive layer or the stress concentration effect of the attack. This study was conducted to quantify the effects of varying degrees of surface intergranular attack on the fatigue properties of the material. Fatigue specimens were machined from actual components taken from inventory and from fielded components and were subsequently categorized into four groups which described the degree or severity of attack based on appearance and depth measurement: none, light, moderate, and heavy. Fatigue test data showed a direct relationship between the number of cycles to failure and the severity of surface intergranular attack. ARL recommended to control the amount of surface intergranular attack or to remove it altogether with a light sanding operation.				
14. SUBJECT TERMS AM355, stainless steel, fatigue, pickling			15. NUMBER OF PAGES 47	
			16. PRICE CODE	
17. SECURITY CLASSIFICATION OF REPORT UNCLASSIFIED	18. SECURITY CLASSIFICATION OF THIS PAGE UNCLASSIFIED	19. SECURITY CLASSIFICATION OF ABSTRACT UNCLASSIFIED	20. LIMITATION OF ABSTRACT UL	

INTENTIONALLY LEFT BLANK.

ACKNOWLEDGMENTS

The authors would like to acknowledge Brad Waterson, Worcester Polytechnic Institute, Worcester, MA, for making significant contributions in acquiring the data expressed within this report.

INTENTIONALLY LEFT BLANK.

TABLE OF CONTENTS

	<u>Page</u>
ACKNOWLEDGMENTS	iii
LIST OF FIGURES	vii
LIST OF TABLES	ix
1. INTRODUCTION	1
2. BACKGROUND	1
3. TEST PLAN	1
4. OPTICAL MICROSCOPY	4
5. SCANNING ELECTRON MICROSCOPY	5
6. FATIGUE AND TENSILE RESULTS	6
7. DISCUSSION	14
8. CONCLUSIONS	15
9. RECOMMENDATIONS	15
DISTRIBUTION LIST	41

INTENTIONALLY LEFT BLANK.

LIST OF FIGURES

<u>Figure</u>	<u>Page</u>
1. SEM fractograph of 11L from SP #7888 showing an edge origin. Mag. 250×.	16
2. SEM fractograph of 11L from SP #7888 showing edge scratches. Mag. 250×.	16
3. SEM fractograph of SP #7888 11L showing the scratch root origin. Mag. 1000×.	17
4. SEM fractograph of SP #7888 11L showing lack of intergranular edge. Mag. 750×.	17
5. SEM fractograph of 10L from SP #6800 showing thumbnail origin. Mag. 50×.	18
6. SEM fractograph of SP #6800 10L showing the origin. Mag. 250×.	18
7. SEM fractograph of SP #6800 10L showing the surface pit origin. Mag. 250×.	19
8. SEM fractograph of SP #6800 10L showing lack of intergranular edge. Mag. 1000×.	19
9. SEM fractograph of Trial R12 showing an edge origin. Mag. 250×.	20
10. SEM fractograph of Trial R12 showing edge scratches. Mag. 250×.	20
11. SEM fractograph of Trial R12 showing an edge scratch origin. Mag. 1000×.	21
12. SEM fractograph of Trial R12 showing fatigue by edge intergranular. Mag. 100×.	21
13. SEM fractograph of Trial R12 showing removed grains on edge. Mag. 750×.	22
14. SEM fractograph of low-cost AR showing surface failure origin. Mag. 250×.	22
15. SEM fractograph of low-cost AR showing location of surface origin. Mag. 100×.	23
16. SEM fractograph of low-cost AR showing intergranular at origin. Mag. 1000×.	23
17. SEM fractograph of low-cost AR intergranular attack near the origin. Mag. 500×.	24
18. SEM fractograph of low-cost AR intergranular morphology at origin. Mag. 3000×.	24
19. SEM fractograph of low-cost AR removed edge grains and secondary cracking origin. Mag. 500×.	25
20. AM355 axial fatigue test - S-N curve; $K_t = 1$; $T = 0.014$; $G = 0.660$; $R = 0.05$	26
21. AM355 axial fatigue test - S-N curve; $K_t = 1$; $T = 0.014$; $G = 0.660$; $R = 0.05$; best-fit curves.	27

<u>Figure</u>	<u>Page</u>
22. AM355 axial fatigue test - S-N curve; $K_t = 1$; $T = 0.014$; $G = 0.660$; $R = 0.05$; trial.	28
23. AM355 axial fatigue test - S-N curve; $K_t = 1$; $T = 0.014$; $G = 0.660$; $R = 0.05$; trial best fit.	29
24. AM355 axial fatigue test - S-N curve; $K_t = 1$; $T = 0.014$; $G = 0.660$; $R = 0.05$; KSD.	30
25. AM355 axial fatigue test - S-N curve; $K_t = 1$; $T = 0.014$; $G = 0.660$; $R = 0.05$; KSD best fit.	31
26. AM355 axial fatigue test - S-N curve; $K_t = 1$; $T = 0.014$; $G = 0.660$; $R = 0.05$; SP #6800.	32
27. AM355 axial fatigue test - S-N curve; $K_t = 1$; $T = 0.014$; $G = 0.660$; $R = 0.05$; SP #6800 best fit.	33
28. AM355 axial fatigue test - S-N curve; $K_t = 1$; $T = 0.014$; $G = 0.660$; $R = 0.05$; SP #7888.	34
29. AM355 axial fatigue test - S-N curve; $K_t = 1$; $T = 0.014$; $G = 0.660$; $R = 0.05$; SP #7888 best fit.	35
30. AM355 axial fatigue test - S-N curve; $K_t = 1$; $T = 0.014$; $G = 0.660$; $R = 0.05$; least-squares regression fit.	36
31. Least-squares regression fit.	37
32. AM355 axial fatigue test - S-N curve; $K_t = 1$; $T = 0.014$; $G = 0.660$; $R = 0.05$; power law fit.	38
33. Power law fit.	39

LIST OF TABLES

<u>Table</u>	<u>Page</u>
1. Laminate Material Test Plan	2
2. Laminate Measurement Data	3
3. Laminate Failure Locations	4
4. Laminate Fatigue Testing Results	7
5. Best-Fit Approximations	8
6. Laminate Least-Squares Regression Fit	13
7. Laminate Mechanical Test Data	14

INTENTIONALLY LEFT BLANK.

1. INTRODUCTION

The purpose of this study was to determine if the fatigue properties of AM355 stainless steel are adversely affected by an intergranular surface attack caused by "pickling" during primary material processing.

2. BACKGROUND

The U.S. Army Aviation and Troop Command (ATCOM) visited the KSD Corporation in response to a surface condition observed on Apache strap pack laminate material, AM355 stainless steel. The material contained small black spots, which appeared during the manufacturing of the strap pack. As a result of this visit, ATCOM requested an analysis of these anomalies from the Materials Directorate of the U.S. Army Research Laboratory (ARL). ARL concluded that the anomalies were caused by entrapped particles on the surface that fretted during manufacturing operations, causing the black spots. The particles had been lodged within areas of surface intergranular attack. As a direct result of that analysis,¹ ATCOM requested ARL to investigate the intergranular surface attack that was the precursor and probable root-cause of the surface anomaly in more detail. ARL was informed that this condition was inherent to the primary processing of AM355 by Allegheny Ludlum and existed on the material before the assembly of the strap pack laminates. Further investigation revealed that the surface intergranular attack on the AM355 laminate material was most likely the result of a prior pickling operation performed during primary processing of the material. The severity of the intergranular attack was not observed during prior ARL analyses (although a similar condition on a much lesser scale was detected on previously inspected strap packs), and its consequences were not known. Until recently, this condition was being removed from some strap packs by a surface finishing operation performed by McDonnell Douglas Helicopter Systems (MDHS). ARL proceeded to perform fatigue and tensile testing of the AM355 laminate material to explore the effects of the surface intergranular attack. A detailed test plan was formulated including material received by ARL from previous investigations of the Main Rotor Strap Pack.

3. TEST PLAN

The test plan included selecting material with varying degrees of attack, including heavy attack, moderate to heavy attack, moderate attack, and only slightly attacked to void of attack. ARL received three sets of

¹Grendahl, S., and V. K. Champagne. "Analysis of AH-64 Apache Strap Pack Laminate Surface Anomalies." U.S. Army Research Laboratory, 26 October 1995.

laminates upon which fatigue and tensile tests were to be performed. The material was designated as "KSD" from KSD corporation, "Trial" from MDHS, and "Low Cost," also from MDHS (that consisted of unprocessed laminates—meaning not reamed, end-milled, or edge broken). In addition, laminates were tested from two strap packs previously received by ARL during an unrelated investigation. Strap pack laminates were taken from SP #6800, that had 614 prior service hours, and from SP #7888, that had 248 prior service hours. These strap laminates were selected to represent "virgin" material since they had few flight hours and thus limited internal mechanical damage. Table 1 outlines the test plan created to assess the effects of the intergranular surface condition on the tensile and fatigue properties of the material.

Table 1. Laminate Material Test Plan

Material	IG Condition	Fatigue (Specs.)	Tensile (Specs.)
KSD	Moderate-Heavy	10	3
Trial	Moderate	16	2
Low Cost	Heavy	2	1
SP #6800	Very Light - None	7	1
SP #7888	Very Light - None	7	1

Each specimen was precisely measured with a Mitutoyo Mikematic Micrometer Model #MK 100E. The results of these measurements are presented in Table 2. ARL was provided with baseline cyclic fatigue curves for the AM355 material. The results of the testing can be observed in tabular form in Table 4 and in graphical form in Figures 20–29.

Table 2. Laminate Measurement Data

Specimen	Thickness					Average	Width					Average	Cross-Sec. Area
TR 1	0.01400	0.01405	0.01410	0.01410	0.01410	0.01407	0.66100	0.66110	0.66105	0.66115	0.66110	0.66108	0.0093014
TL1	0.01415	0.01415	0.01415	0.01415	0.01415	0.01415	0.66060	0.66050	0.66055	0.66060	0.66045	0.66054	0.0093466
TR 2	0.01405	0.01400	0.01405	0.01410	0.01405	0.01405	0.66130	0.66135	0.66140	0.66125	0.66135	0.66133	0.0092917
TL 2	0.01415	0.01415	0.01415	0.01415	0.01415	0.01415	0.66085	0.66110	0.66125	0.66100	0.66120	0.66108	0.0093543
TL5	0.01405	0.01410	0.01415	0.01415	0.01410	0.01411	0.66110	0.66115	0.66105	0.66100	0.66115	0.66109	0.0093280
TR 5	0.01410	0.01415	0.01405	0.01410	0.01410	0.01410	0.66095	0.66085	0.66105	0.66100	0.66090	0.66095	0.0093194
TR 6	0.01400	0.01405	0.01400	0.01410	0.01405	0.01404	0.66100	0.66105	0.66120	0.66100	0.66110	0.66107	0.0092814
TL 6	0.01405	0.01405	0.01410	0.01410	0.01405	0.01407	0.66085	0.66100	0.66090	0.66120	0.66110	0.66093	0.0092993
TL7	0.01410	0.01410	0.01405	0.01405	0.01405	0.01407	0.66100	0.66075	0.66095	0.66085	0.66085	0.66108	0.0093014
TR 7	0.01410	0.01410	0.01405	0.01410	0.01415	0.01410	0.66105	0.66095	0.66100	0.66090	0.66095	0.66097	0.0093197
TR 11	0.01410	0.01405	0.01410	0.01410	0.01410	0.01409	0.66070	0.66080	0.66075	0.66075	0.66070	0.66088	0.0093118
TL11	0.01415	0.01415	0.01415	0.01415	0.01410	0.01414	0.66100	0.66105	0.66095	0.66115	0.66120	0.66074	0.0093429
TR 12	0.01405	0.01405	0.01400	0.01405	0.01405	0.01404	0.66085	0.66090	0.66095	0.66080	0.66080	0.66101	0.0092806
TL 12	0.01415	0.01415	0.01410	0.01415	0.01415	0.01414	0.66100	0.66050	0.66085	0.66095	0.66060	0.66117	0.0093489
TL 14	0.01410	0.01410	0.01405	0.01410	0.01410	0.01409	0.66120	0.66130	0.66130	0.66125	0.66115	0.66083	0.0093111
TR 19	0.01400	0.01405	0.01405	0.01405	0.01410	0.01403	0.66100	0.66050	0.66085	0.66095	0.66060	0.66078	0.0092707
TL 19	0.01410	0.01410	0.01405	0.01410	0.01415	0.01410	0.66120	0.66130	0.66130	0.66125	0.66115	0.66124	0.0093235
TR 21	0.01410	0.01405	0.01410	0.01415	0.01405	0.01409	0.66100	0.66105	0.66090	0.66095	0.66095	0.66097	0.0093131
TL 21	0.01405	0.01405	0.01405	0.01405	0.01410	0.01406	0.66090	0.66105	0.66115	0.66100	0.66120	0.66106	0.0092945
7888 L 11	0.01410	0.01410	0.01410	0.01410	0.01410	0.01410	0.66130	0.66025	0.66040	0.66030	0.66025	0.66030	0.0093102
7888 R 11	0.01405	0.01410	0.01410	0.01410	0.01415	0.01410	0.65980	0.65960	0.65940	0.65965	0.65955	0.65960	0.0093004
7888 L 12	0.01420	0.01420	0.01415	0.01420	0.01420	0.01419	0.66030	0.66050	0.66035	0.66040	0.66020	0.66035	0.0093704
7888 R 12	0.01420	0.01425	0.01425	0.01420	0.01415	0.01421	0.66030	0.66025	0.66040	0.66025	0.66040	0.66032	0.0093831
7888 L 13	0.01415	0.01415	0.01415	0.01415	0.01420	0.01416	0.66010	0.66005	0.66010	0.66015	0.65980	0.66004	0.0093462
7888 R 13	0.01425	0.01420	0.01420	0.01425	0.01425	0.01423	0.65995	0.65975	0.65960	0.65980	0.65965	0.65975	0.0093882
6800 L 9-1	0.01400	0.01400	0.01400	0.01405	0.01400	0.01401	0.66060	0.66050	0.66055	0.66065	0.66060	0.66058	0.0092547
6800 L 9-2	0.01400	0.01405	0.01405	0.01400	0.01400	0.01402	0.66045	0.66050	0.66055	0.66040	0.66045	0.66047	0.0092598
6800 L 10	0.01400	0.01400	0.01400	0.01400	0.01400	0.01400	0.66075	0.66060	0.66080	0.66080	0.66060	0.66071	0.0092499
6800 R 10	0.01415	0.01405	0.01405	0.01400	0.01400	0.01405	0.65985	0.65990	0.66010	0.66005	0.65995	0.65997	0.0092726
6800 L 11	0.01400	0.01400	0.01420	0.01415	0.01400	0.01407	0.66080	0.66090	0.66095	0.66080	0.66105	0.66090	0.0092989
6800 R 11	0.01400	0.01400	0.01400	0.01410	0.01405	0.01403	0.65990	0.65985	0.65980	0.65995	0.65010	0.65992	0.0092587
6800 L 13	0.01400	0.01405	0.01405	0.01400	0.01400	0.01402	0.66045	0.66050	0.66070	0.66070	0.66075	0.66062	0.0092619
6800 L13-2	0.01395	0.01395	0.01395	0.01390	0.01395	0.01399	0.65960	0.65970	0.65950	0.65975	0.65995	0.65970	0.0092292
LCAL	0.01455	0.01455	0.01455	0.01455	0.01450	0.01454	0.66075	0.66080	0.66100	0.66085	0.66105	0.66089	0.0096093
LCBL	0.01465	0.01460	0.01465	0.01460	0.01465	0.01463	0.66110	0.66130	0.66150	0.66135	0.66140	0.66133	0.0096753
LCAR	0.01470	0.01470	0.01470	0.01460	0.01465	0.01467	0.66140	0.66135	0.66155	0.66145	0.66140	0.66143	0.0097032
KSD AR	0.01405	0.01405	0.01400	0.01400	0.01405	0.01403	0.66160	0.66170	0.66165	0.66140	0.66150	0.66157	0.0092818
KSD BL	0.01405	0.01405	0.01405	0.01410	0.01410	0.01407	0.66260	0.66270	0.66280	0.66260	0.66280	0.66270	0.0093242
KSD BR-1	0.01400	0.01405	0.01405	0.01405	0.01400	0.01403	0.66290	0.66280	0.66275	0.66280	0.66290	0.66283	0.0092995
KSD BR-2	0.01405	0.01400	0.01400	0.01400	0.01400	0.01401	0.66095	0.66085	0.66080	0.66100	0.66090	0.66090	0.0092592
KSD CL	0.01400	0.01400	0.01395	0.01400	0.01400	0.01399	0.66380	0.66400	0.66415	0.66380	0.66370	0.66376	0.0092860
KSD CR-1	0.01400	0.01400	0.01400	0.01405	0.01400	0.01401	0.66250	0.66260	0.66225	0.66230	0.66245	0.66247	0.0092812
KSD CR-2	0.01405	0.01400	0.01400	0.01390	0.01400	0.01399	0.66100	0.66085	0.66080	0.66095	0.66085	0.66089	0.0092459
KSD DL	0.01400	0.01400	0.01400	0.01400	0.01400	0.01400	0.66140	0.66120	0.66105	0.66095	0.66095	0.66111	0.0092555
KSD DR-1	0.01390	0.01395	0.01390	0.01395	0.01390	0.01393	0.66175	0.66180	0.66170	0.66185	0.66180	0.66179	0.0092187
KSD DR-2	0.01395	0.01400	0.01400	0.01405	0.01400	0.01401	0.66100	0.66120	0.66135	0.66140	0.66115	0.66122	0.0092637

4. OPTICAL MICROSCOPY

The fractured halves from the fatigue and tensile testing were optically examined. The fracture origins were determined to be from either edge or surface flaws. A listing is presented in Table 3.

Table 3. Laminate Failure Locations

Specimen	Failure Location
TR 1	not failed
TL1	edge
TR 2	not failed
TL 2	edge
TL5	edge
TR 6	not failed
TL 6	edge
TL7	not failed
TR 11	edge
TL11	edge
TR 12	edge
TL 12	edge
TL 14	edge
TR 19	edge
TL 19	edge
TR 21	not failed
TL 21	not failed
7888 L 11	edge
7888 R 11	edge
7888 L 12	edge
7888 R 12	edge
7888 L 13	not failed
7888 R 13	edge
6800 L 10	surface pit
6800 R 10	edge
6800 L 11	not failed
6800 R 11	edge
LCAL	not failed
LCBL	not failed
LCAR	surface
KSD AR	edge
KSD BL	not failed
KSD BR-1	edge
KSD BR-2	edge
KSD CL	not failed
KSD CR-1	edge
KSD CR-2	edge
KSD DL	edge
KSD DR-1	edge
KSD DR-2	edge

5. SCANNING ELECTRON MICROSCOPY

Scanning electron microscopy was used to determine the exact nature of failure and location of the fatigue origin(s). The specimens failed predominantly from edge defects. The edge finishing performed on the specimens allowed for scratches perpendicular to the specimen length. For the specimens that failed from the edge, these scratches were the origin of fracture, as expected. Figure 1 shows specimen 11L from Strap Pack #7888 with an edge fracture origin (arrow denotes origin). Further investigation revealed scratches on the edge as a result of the finishing procedure, as shown in Figure 2. Upon closer examination, it was observed that the root of a scratch on the edge of the specimen was the origin of fracture. The origin is depicted at higher magnification in Figure 3. Specimens from Strap Pack #7888 did not display any intergranular attack of the surface, and consequently, the edge of the fatigue specimen did not contain any intergranular morphology along its edges. The surface edge of specimen #7888 11L can be observed in Figure 4.

Figure 5 shows specimen 10L from Strap Pack #6800. A "thumbnail" crack region can be seen containing radial lines that indicate the origin of the fracture. The origin is shown at higher magnification in Figure 6. Since both Strap Packs #7888 and #6800 had seen prior service, it was expected that pitting and subsequent surface failures would be observed. Specimen 10L from #6800 failed from a surface pit as depicted in Figure 7. There was no intergranular fracture morphology along the edges of the specimens from Strap Pack #6800. This was expected, since Strap Pack #6800 had minimal to no surface intergranular attack. Figure 8 depicts the edge of specimen 10L from #6800 at high magnification. For comparison, the failures of the specimens with some surface intergranular attack were examined.

Figure 9 shows the edge failure of "Trial" Strap Pack specimen R12 (arrow denotes origin). This edge failure was caused by surface scratches induced during the edge finishing process, shown in Figure 10 and at higher magnification in Figure 11. However, the "Trial" strap-pack laminates contained characteristics near the surface not witnessed on the strap packs that had experienced prior service (#7888 and #6800). The intergranular attack of the surface of these specimens (categorized as moderate attack) allowed the fatigue crack front to progress along an intergranular network near the surface. Figure 12 shows the fatigue crack following the intergranular network near the surface of the specimens (arrows denote intergranular morphology along edges).

Figure 13 depicts the edge of specimen "Trial" R12. It can clearly be seen that the intergranular surface attack allows the crack to progress in an intergranular mode near the surface. It can be observed in Figure 13 that a few grains were removed entirely as the crack progressed around them. There were also significant secondary cracks on the surface of the specimen adjacent to the main crack front.

Figure 14 shows the origin area on specimen AR from the Strap Pack labeled "low cost." The intergranular condition of these laminates was the worst or the deepest surface attack observed. This specimen failed from a surface flaw. Figure 15 shows the proximity of the surface flaw origin to the nearest edge. Closer examination revealed an intergranular morphology at the origin (shown in Figure 16). The surface intergranular condition near the origin is shown in Figure 17. The depth and severity of this attack can easily be observed. The intergranular morphology at the origin is depicted at high magnification in Figure 18. The effect of the heavy intergranular surface attack can be observed in Figure 19 as removed grains and severe secondary cracking are clearly evident as well as intergranular morphology along the edge. The specimens that did not contain this intergranular network did not have the crack front progressing in an intergranular mode near the surface. The crack front progressed by a transgranular mode until transitioning to complete ductility.

6. FATIGUE AND TENSILE RESULTS

The results of the fatigue tests are presented in Table 4 and in graphical format in Figures 20–33. Figures 20–29 show the data plotted with "best-fit" approximations according to the equation $y = (a + b \ln(x) + c/x^2)$, which was acquired from curve-fitting software. A least-squares regression fit is applied in Figures 30 and 31. Finally, a power law fit is applied to the data in Figures 32 and 33.

The "best-fit" approximations can be previewed in Table 5.

Table 4. Laminate Fatigue Testing Results

Specimen Designation	Scribe Designation	Cyclic Stress Amplitude	Cross-Sectional Area	Projected Loads (Pounds)			Cyclic Stress	Cycles To Failure
				Max.	Min.	Mean		
6800 9L-1	9L-1	67.5	0.0092547	1314.3	65.7	690	624.4	55565
6800 9L-2	9L-2	67.4	0.0092598	1314.3	65.7	690	624.4	47986
6800 L 10	L 10	74.9	0.0092499	1459	73.0	766.0	693	88805
6800 R 10	R 10	69.8	0.0092726	1362.0	68.0	715.0	647	71278
6800 R 11	R 11	79.8	0.0092587	1552.0	77.6	814.8	814.8	37649
6800 13L-1	13L-1	64.9	0.0092619	1265.4	62.9	664.2	601.3	3 Million
6800 13L-2	13L-2	65	0.0092292	1264.0	62.8	663.6	600.6	3 Million
7888 11 L	11 L	71.9	0.0093102	1408.5	70.4	739.3	669.2	43237
7888 11 R	11 R	79.5	0.0093004	1552.0	77.6	815.0	739.2	23394
7888 12 L	12 L	71.5	0.0093704	1409.7	70.5	740.1	669.6	99601
7888 12 R	12 R	73.8	0.0093831	1459.0	73.0	766.0	693	40925
7888 13 L	13 L	69.2	0.0093462	1362.0	68.0	715.0	647	3 Million
7888 13 R	13 R	71.3	0.0093882	1409.7	70.5	740.1	669.6	87210
KSD AR	AR	64.9	0.0092818	1269.0	63.4	665.3	602.8	165352
KSD BL	BL	64.6	0.0093242	1269.0	63.4	665.3	602.8	3 Million
KSD BR-1	BR-1	72.2	0.0092995	1413.2	70.7	742.0	671.3	60221
KSD BR-2	BR-2	86.9	0.0092592	1649.1	85.9	889.0	804.6	17101
KSD CL	CL	62.7	0.0092860	1225.7	80.9	643.3	582.4	3 Million
KSD CR-1	CR-1	77	0.0092812	1505.5	75.1	790.3	715.2	35513
KSD CR-2	CR-2	67.5	0.0092459	1314.8	66.0	690.4	624.4	28540
KSD DL	DL	67.5	0.0092555	1314.8	66.0	690.4	624.4	84361
KSD DR-1	DR-1	68	0.0092187	1319.2	66.2	692.7	626.5	56138
KSD DR-2	DR-2	65.1	0.0092637	1269.0	63.4	665.3	602.8	291466
LC 802757AL	LCAL	untested	0.0096093					
LC 802757AR	LCAR	66.7	0.0097032	1362.0	68.0	715.0	647	53190
LC 802757BL	LCBL	57.3	0.0096753	1167.0	58.4	612.8	554.4	3 Million
Trial L1	TL1	69.2	0.0093466	1362.0	68.0	715.0	647	44611
Trial R1	TR1	57	0.0093014	119.0	56.4	587.2	531	3 Million
Trial L2	TL2	64.3	0.0093543	1266.3	63.3	665.0	601.5	70422
Trial R2	TR2	64.7	0.0092917	1266.3	63.3	665.0	601.5	3 Million
Trial L5	TL5	66.9	0.0093280	1314.3	65.7	690.0	624.6	87941
Trial R5	TR5	62	0.0093194	1217.0	60.9	639.0	578	93117
Trial L6	TL6	62.1	0.0092993	1217.0	60.9	639.0	578	62477
Trial R6	TR6	54.2	0.0092814	1069.9	53.6	561.3	508.2	3 Million
Trial L7	TL7	59.7	0.0093014	1168.0	58.3	613.3	555	3 Million
Trial R7	TR7	62	0.0093197	1217.0	60.9	639.0	578	137717
Trial L11	TL11	79.6	0.0092806	1552.0	77.6	815.0	739.2	31960
Trial R11	TR11	59.5	0.0093118	1167.0	58.4	612.8	554.4	155895
Trial R12	TR12	82	0.0093489	1595.0	250.0	916.8	???	42218
Trial L14	TL14	89.3	0.0093111	1750.7	87.5	919.1	831.6	10986
Trial L19	TL19	79.3	0.0093235	1552.0	77.6	815.0	739.2	66804
Trial R19	TR19	69.8	0.0092707	1362.0	68.0	715.0	647	77780

Table 5. Best-Fit Approximations

Trial Data		XY Pt #	Cycles	Cyclic Stress Amp.	Y Predicted	Y Residual	Y % Residual	95% Confidence Limits		95% Prediction Limits	
Date	Apr 3, 1996	1	10986	89.3	90.5238249	-1.22382489	-1.3704646	76.91306447	104.134585	71.22826496	109.819385
Time	4:16 PM	2	31960	79.6	72.8093083	6.7906917	8.53101972	68.05969696	77.5589196	58.33088844	87.2877282
XY Points	16	3	42218	82	71.1670484	10.8329516	13.2109166	66.5806865	75.753428	56.74135209	85.5927446
XY Minimum	10986	4	44611	69.2	70.8902181	-1.69021814	-2.44251176	66.3400015	75.4404348	56.47597847	85.3044578
XY Maximum	3000000	5	62447	62.1	69.4242063	-7.32420627	-11.794213	65.12709624	73.7213163	55.08785428	83.7605583
X Range	2989014	6	66804	79.3	69.1642139	10.1357861	12.7815713	64.92201239	73.4064155	54.84422414	83.4842037
X Mean	805118.63	7	70422	64.3	68.966645	-4.66664495	-7.25761268	64.76759483	73.1656951	54.65937912	83.2739108
X StdDev	1309262	8	77780	69.8	68.6062348	1.19376524	1.71026538	64.48808451	72.724385	54.32250292	82.8899666
X Median	82860.5	9	87941	66.9	68.1787917	-1.27879168	-1.91149728	64.15784676	72.1997366	53.9227813	82.4348021
X @ Ymin	3000000	10	93117	62	67.985274	-5.985274	-9.65366775	64.00782825	71.9627198	53.74147155	82.2290765
X @ Ymax	10986	11	137717	62	66.727175	-4.72717499	-7.62447579	62.99399558	70.4603544	52.54964127	80.9047087
X @ Y Range	2989014	12	155895	59.5	66.3451166	-6.84511658	-11.5043976	62.66272769	70.0275055	52.1808721	80.5093611
Xavg @ Yma	10986	13	3E+06	57	57.7029858	-0.70298579	-1.2333084	50.97414408	64.4318275	42.46017947	72.9457921
X @ 50Y	179979.82	14	3E+06	54.2	57.7029858	-3.50298579	-6.40307341	50.97414408	64.4318275	42.46017947	72.9457921
X @ 50Y	0	15	3E+06	59.7	57.7029858	-1.99701421	-3.43508243	50.97414408	64.4318275	42.46017947	72.9457921
X @ 25Y	-1356704	16	3E+06	64.7	57.7029858	6.99701421	10.8145506	50.97414408	64.4318275	42.46017947	72.9457921
X @ 75Y	-17336.26										
Xwavenmin	3000000			Equation #	75						
Xwavenmax	10986			Equation	$y=(a+b \ln(x)+c/x^2)$						
Xwave Rang	5978028			r ²	0.65330832022						
Y Minimum	54.2			Fit StdErr	6.32317907						
Y Maximum	89.3			F-stat	12.2486587						
Y Range	35.1			Confidence	95						
Y Mean	67.6			A	100.873859						
Y StdDev	9.9974663			A StdErr	12.3988696						
Y Median	64.5			A t	8.13573032						
Y @ Xmin	89.3			A Conf Limits	74.0547808						
Y @ Xmax	64.7			B	127.692937						
Y @ X Range	24.6			B	-2.8946453						
F1				B StdErr	0.9990798						
F2				B t	-2.8973114						
F3				B Conf Limits	-5.055681						
				C	-0.7336096						
				C	2001419022						
				C StdErr	905851481						
				C t	2.20943396						
				C Conf Limits	42038645						
					3960799399						

Table 5. Best-Fit Approximations (continued)

Table 5. Best-Fit Approximations (continued)

Table 5. Best-Fit Approximations (continued)

SP 7888 Data																		
Date	Apr 3, 1996	XY Pt #	Cycles	Cyclic Stress Amp.	Y Predicted	Y Residual	Y % Residual	95% Confidence Limits										
Time	3:53 PM	1	23394	79.5	79.29240429	0.20759571	0.26112668	76.69187029										81.8929383
XY Points		2	40925	73.8	73.46132158	0.33867842	0.45891384	72.14551735										74.7771258
XY Minimum	23394	3	43237	71.9	73.15788799	-1.25788799	-1.74949651	71.82547342										74.4903026
XY Maximum	2758892	4	87210	71.3	71.07374405	0.22625595	0.31732952	69.59244974										72.5550384
X Range	2735498	5	99601	71.5	70.88889903	0.61110097	0.85468667	69.41440419										72.3633939
X Mean	508876.5	6	3E+06	69.2	69.32574305	-0.12574305	-0.18170961	66.65739861										71.9940875
X StdDev	1102666.843																	
X Median	65223.5			Equation #	75													
X@Ymin	2758892			Equation	$Y=(a+b\ln(x)+c/x^2)$													
X@Ymax	23394			r2	0.965700576268													
X@Y Range	2735498			Fit StdErr	0.852550819													
Xavg@Ymax	23394			F-stat	42.23251317													
X@50Y	39945.37031			Confidence	95													
Xlr@50Y	0			A	74.24178267													
Xrt@50Y	0			A StdErr	3.565218021													
X@25Y	69868.27089			A t	20.82391097													
X@75Y	33393.63848			A Conflimits	62.97983665													
Xwavenin	2758892				85.50372869													
Xwavenax	23394			B	-0.331525958													
Xwave Range	5470996			B StdErr	0.286245771													
Y Minimum	69.2			B t	-1.158186394													
Y Maximum	79.5			B Conflimits	-1.235729966													
Y Range	10.3				0.572678051													
Y Mean	72.86666667			C	4589401917													
Y StdDev	3.565763125			C StdErr	720339021.3													
Y Median	71.7			C t	6.371169381													
Y@Xmin	79.5			C Conflimits	2313967672													
Y@Xmax	69.2				6864836162													
Y@X Range	10.3																	
F1																		
F2																		
F3																		

The power law fits used can be previewed below:

- Power Law Fit for Trial Data

Fit 6: Power, $\log(Y) = B * \log(X) + A$

Equation: $\log(Y) = -.0569387 * \log(X) + 4.88673$

Alternate equation:

$Y = \text{pow}(X, -.0569387) * 132.519$

Number of data points used = 16

Average $\log(X) = 11.9926$

Average $\log(Y) = 4.20389$

Regression sum of squares = 0.165529

Residual sum of squares = 0.137835

Coef. of determination, $R^2 = 0.545645$

Residual mean square, $\hat{\Sigma}^2 = 0.00984536$

- Power Law Fit for KSD Data

Fit 8: Power, $\log(Y) = B * \log(X) + A$

Equation: $\log(Y) = -0.0387338 * \log(X) + 4.69652$

Alternate equation:

$Y = \text{pow}(X, -0.0387338) * 109.566$

Number of data points used = 10

Average $\log(X) = 11.8195$

Average $\log(Y) = 4.23871$

Regression sum of squares = 0.0449737

Residual sum of squares = 0.0439293

Coef. of determination, $R^2 = 0.505874$

Residual mean square, $\hat{\Sigma}^2 = 0.00549117$

- Power Law Fit for SP #6800 Data

Fit 7: Power, $\log(Y) = B * \log(X) + A$

Equation: $\log(Y) = -0.025433 * \log(X) + 4.55198$

Alternate equation:

$Y = \text{pow}(X, -0.025433) * 94.8204$

Number of data points used = 7

Average $\log(X) = 12.091$

Average $\log(Y) = 4.24447$

Regression sum of squares = 0.0147251

Residual sum of squares = 0.0208858

Coef. of determination, $R^2 = 0.413501$

Residual mean square, $\hat{\Sigma}^2 = 0.00417716$

● Power Law Fit for SP #7888 Data

Fit 9: Power, $\log(Y) = B * \log(X) + A$

Equation: $\log(Y) = -0.0201549 * \log(X) + 4.51968$

Alternate equation:

$Y = \text{pow}(X, -0.0201549) * 91.8061$

Number of data points used = 6

Average $\log(X) = 11.5116$

Average $\log(Y) = 4.28766$

Regression sum of squares = 0.00594523

Residual sum of squares = 0.005477

Coef. of determination, $R^2 = 0.520496$

Residual mean square, $\hat{\Sigma}^2 = 0.00136925$

The least-squares regression used can be previewed in Table 6.

Table 6. Laminate Least-Squares Regression Fit

Specimen Designation	Scribe Desig.	Cyclic Stress Amplitude (KSI)	Cycles to Failure	S^2	SlogN	logN		Actual Stress	Projected Fatigue Life
6800 R11	R11	79.8	37649	6368.04	365.145125	4.57575345	Sum (LogN)	36.7573	A1= 11.957311
6800 L10	L10	74.9	88805	5610.01	370.637963	4.94843742	Sum(S^2)	34386.11	A2= -0.095941
6800 R10	R10	69.8	71278	4872.04	338.736294	4.85295551	Sum(S)	489.3	
6800 9L-1	9L-1	67.5	55565	4556.25	320.274089	4.74480132	Sum(SlogN)	2551.679	
6800 9L-2	9L-2	67.4	47986	4542.76	315.507121	4.68111455	(Sum S)^2	239414.5	
6800 13L-1	13L-1	64.9	3.00E+06	4212.01	420.365169	6.47712125	n	7	
6800 13L-2	13L-2	65	3.00E+06	4225	421.012882	6.47712125			
7888 11R	11R	79.5	23394	6320.25	347.343807	4.36910449	Sum (LogN)	30.0329	A1= 13768235
7888 12R	12R	73.8	40925	5446.44	340.364765	4.61198869	Sum(S^2)	31920.88	A2= 2188.3973
7888 11L	11L	71.9	43237	5169.61	333.318014	4.63585555	Sum(S)	437.2	
7888 12L	12L	71.5	99601	5112.25	357.375854	4.9982637	(Sum S)^2	191143.8	
7888 13R	13R	71.3	87210	5083.69	352.262376	4.94056629	n	6	
7888 13L	13L	69.2	3.00E+06	4788.64	448.216791	6.47712125			
KSD BR-2	BR-2	86.9	17101	7551.61	367.849569	4.23302151	Sum (LogN)	51.33125	A1= 10.310741
KSD CR-1	CR-1	77	35513	5929	350.379827	4.55038736	Sum(S^2)	48984.42	A2= -0.074348
KSD BR-1	BR-1	72.2	60221	5212.84	345.097803	4.77974796	Sum(S)	696.4	
KSD CR-2	CR-2	67.5	28540	4556.25	300.743143	4.45545397	Sum(SlogN)	3538.491	
KSD DL	DL	67.5	84361	4556.25	332.514566	4.92614172	(Sum S)^2	484973	
KSD DR-1	DR-1	68	56138	4624	322.949472	4.74925694	n	10	
KSD AR	AR	64.9	165352	4212.01	338.674773	5.21840945			
KSD BL	BL	64.6	3.00E+06	4173.16	418.422033	6.47712125			
KSD DR-2	DR-2	65.1	291466	4238.01	355.744672	5.4645879			
KSD CL	CL	62.7	3.00E+06	3931.29	406.115503	6.47712125			
Trial 1 L14	TL14	89.3	10986	7974.49	360.846976	4.04083959	Sum (LogN)	83.33301	A1= 9.126935
Trial 1 R12	TR12	82	42218	6724	379.290808	4.62549766	Sum(S^2)	74615.4	A2= -0.057968
Trial 1 L11	TL11	79.6	31960	6336.16	358.566699	4.50460677	Sum(S)	1081.6	
Trial 1 L19	TL19	79.3	66804	6288.49	382.606836	4.82480247	Sum(SlogN)	5546.404	
Trial 1 L1	TL1	69.2	44611	4788.64	321.741384	4.64944196	(Sum S)^2	1169859	
Trial 1 R19	TR19	69.8	77780	4872.04	341.382582	4.89086794	n	16	
Trial 1 L5	TL5	66.9	87941	4475.61	330.766405	4.9441914			
Trial 1 L2	TL2	64.3	70422	4134.49	311.707647	4.84770835			
Trial 1 R2	TR2	64.7	3.00E+06	4186.09	419.069745	6.47712125			
Trial 1 L6	TL6	62.1	62477	3856.41	297.814222	4.79572017			
Trial 1 R5	TR5	62	93117	3844	308.079796	4.96902898			
Trial 1 R7	TR7	62	137717	3844	318.617228	5.13898755			
Trial 1 L7	TL7	59.7	3.00E+06	3564.09	386.684139	6.47712125			
Trial 1 R11	TR11	59.5	155895	3540.25	308.973515	5.19283219			
Trial 1 R1	TR1	57	3.00E+06	3249	369.195912	6.47712125			
Trial 1 R6	TR6	54.2	3.00E+06	2937.64	351.059972	6.47712125			

Least Squares Equations Used

$$\log N = A_1 + A_2 (S)$$

$$A_1 = \frac{\sum \log N \sum (S^2) - \sum S \sum (S \log N)}{n \sum (S^2) - (\sum S)^2}$$

$$A_2 = \frac{n \sum (S \log N) - (\sum S)(\sum \log N)}{n \sum (S^2) - (\sum S)^2}$$

The results of the tensile testing for AM355 are presented in tabular format in Table 7.

Table 7. Laminate Mechanical Test Data

Specimen Designation	Cross-Sectional Area	UTS (KSI)	0.2% Yield Stress (KSI)	% Elongation
LCAR	0.0096	240	194	15.6
LCBL	0.0096	242	227	17.9
TR 4	0.0093	250	189	19.6
TR 20	0.0093	246	185	17.4
TL 4	0.0093	250	179	17.0
TL 20	0.0093	251	198	19.7
6800 R 10	0.0092	253	249	15.4
6800 R 11	0.0092	256	250	15.5
KSD-AL	0.00927	251.3	219.8	24.1
KSD-BL	0.00927	249.7	210.4	24.6
KSD-DL	0.0093	254.8	212.1	23.6

7. DISCUSSION

It can be clearly seen from the optical and electron microscopy results that the surface intergranular condition has an effect on the initiation and progression of a fatigue crack front. The intergranular network of attack on the surface of the material has been measured to be approximately 100–250 μin deep, varying upon the location measured and the coil of material from which the specimens were acquired. The intergranular attack is present on both sides of the material and constitutes approximately 2.5% of the total cross-sectional area (using 175 μin as the average depth of the intergranular surface attack and the fact that the material is only approximately 0.014 in thick). The significance of 2.5% of the cross-sectional area being attacked can be clearly seen in the micrographs and in the fatigue data. The intergranular attack lowers the fatigue life of the material simply because a fatigue crack front can easily follow the intergranular network of attack near the surface, and less energy is needed to propagate the crack. The specimens with no surface intergranular attack failed from either edge scratches or surface pits from service. The specimens with a surface intergranular attack failed mostly from edge scratches. However, specimen "low-cost" AR failed from the surface intergranular attack. These specimens had the most severe intergranular attack. Although this merits further investigation, it must be accepted that severe intergranular attack of the surface of the laminates can initiate fatigue failures. The crack obviously progressed along the intergranular network near

the surface edges of the specimens that exhibited surface intergranular attack. This mode was not evident on the specimens that did not contain significant surface intergranular attack. It would be expected that having an intergranular network (from the intergranular attack) on the surface of the laminates would lower the fatigue life of the material. This was demonstrated in the graphical presentation of the fatigue data. It can clearly be seen in all three fits of the data that the "Trial" and "KSD" specimens have lower overall and projected fatigue lives. It would be interesting to further study the material labeled "low cost," since it would be expected to have the lowest fatigue life because of the severity of its intergranular attack of the surface. The tensile data all fell within the normal values for the material. It appears that the surface intergranular condition does not have a significant effect on the tensile properties of the material.

8. CONCLUSION

The S/N curves generated as a result of fatigue data produced from specimens of AM355 material having intergranular surface attack are lower (2–10-ksi cyclic stress amplitude for similar cycles) than those for similar specimens without this surface attack.

9. RECOMMENDATIONS

The results of this work demonstrate a reduction in fatigue resistance for specimens having an intergranular network of attack of the surface of the material. The effect of the intergranular attack on the fatigue properties needs to be quantified by using material from the same coil (i.e., the same heat treat and surface conditions). Therefore, the material could be tested with the intergranular attack present and with it removed, while all other variables remain constant. Data from a study of this nature could be used to project the fatigue life of material now in service.



Figure 1. SEM fractograph of 11L from SP #7888 showing an edge origin. Mag. 250 \times .

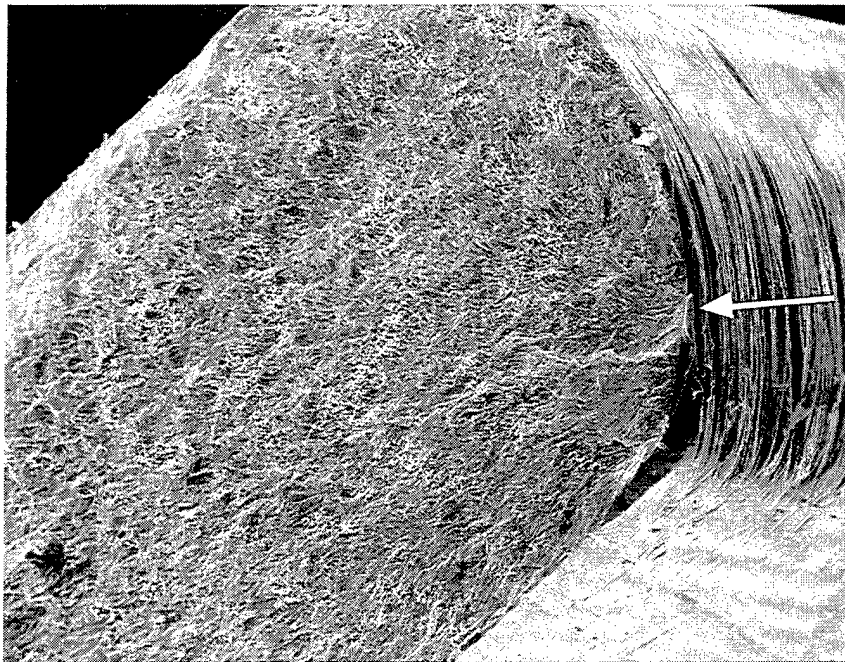


Figure 2. SEM fractograph of 11L from SP #7888 showing edge scratches. Mag. 250 \times .

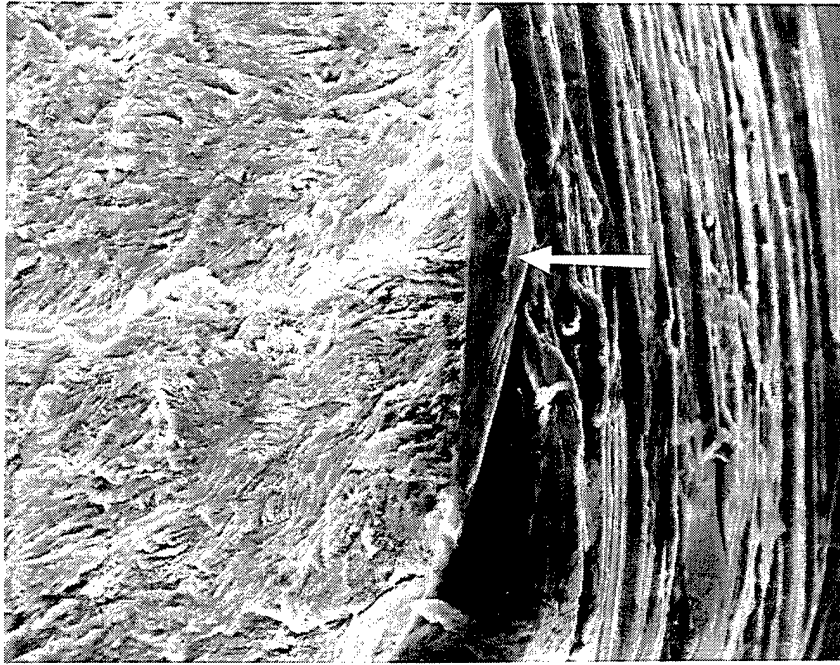


Figure 3. SEM fractograph of SP #7888 11L showing the scratch root origin. Mag. 1000 \times .

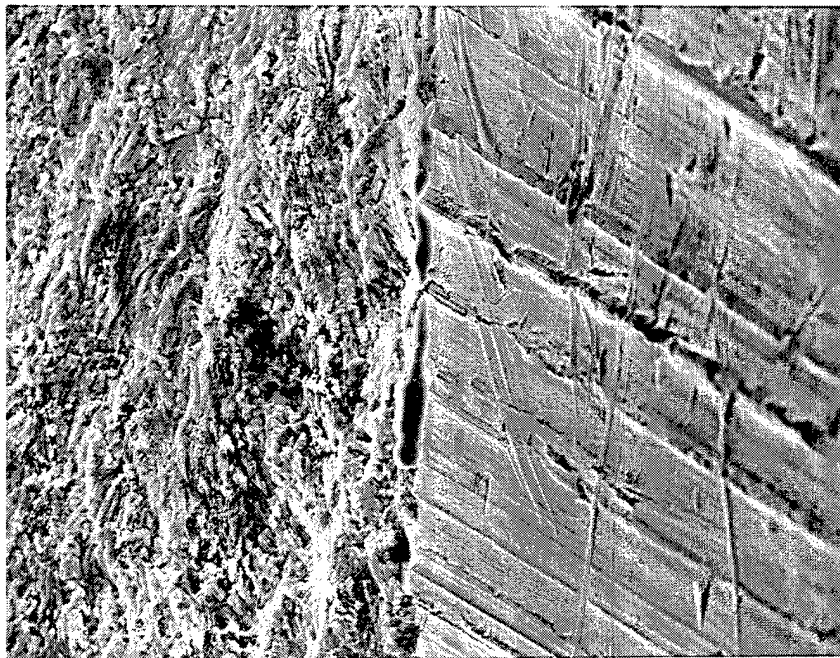


Figure 4. SEM fractograph of SP #7888 11L showing lack of intergranular edge. Mag. 750 \times .

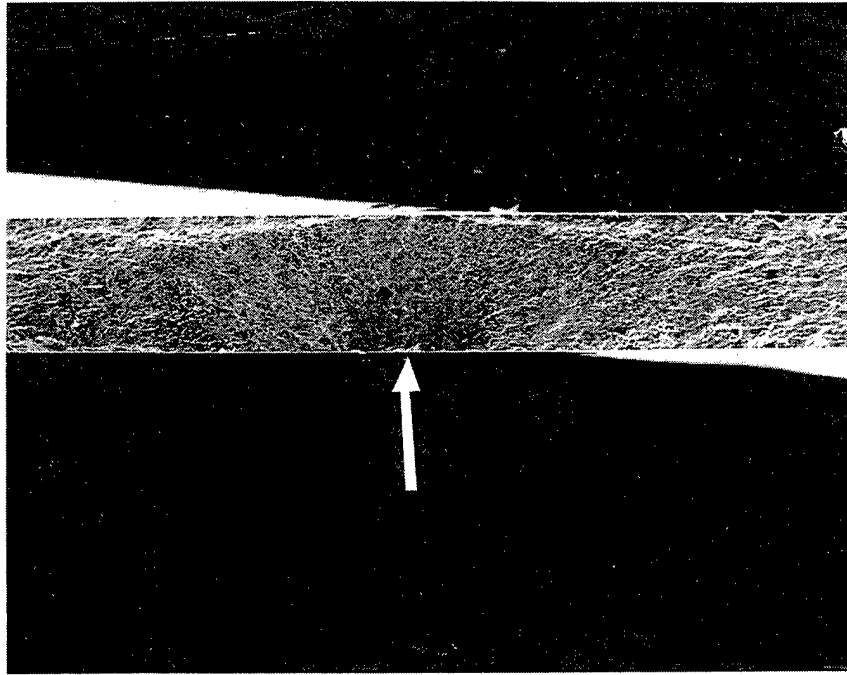


Figure 5. SEM fractograph of 10L from SP #6800 showing thumbnail origin. Mag. 50x.

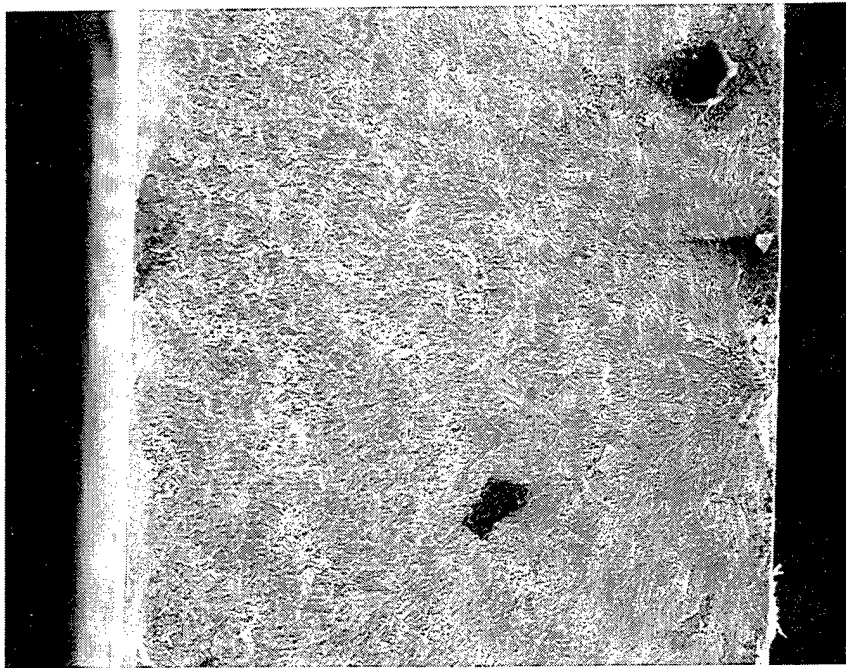


Figure 6. SEM fractograph of SP #6800 10L showing the origin. Mag. 250x.

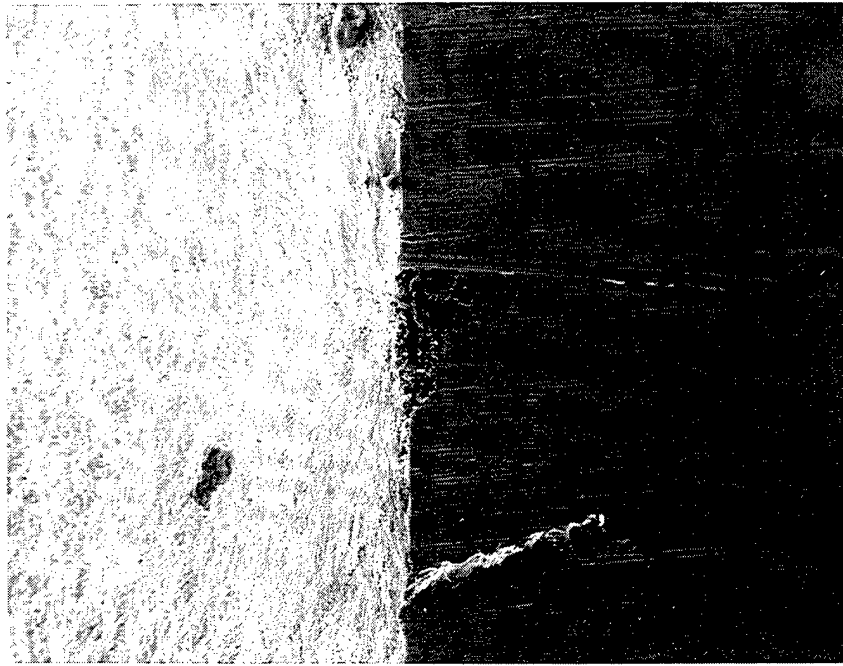


Figure 7. SEM fractograph of SP #6800 10L showing the surface pit origin. Mag. 250 \times .

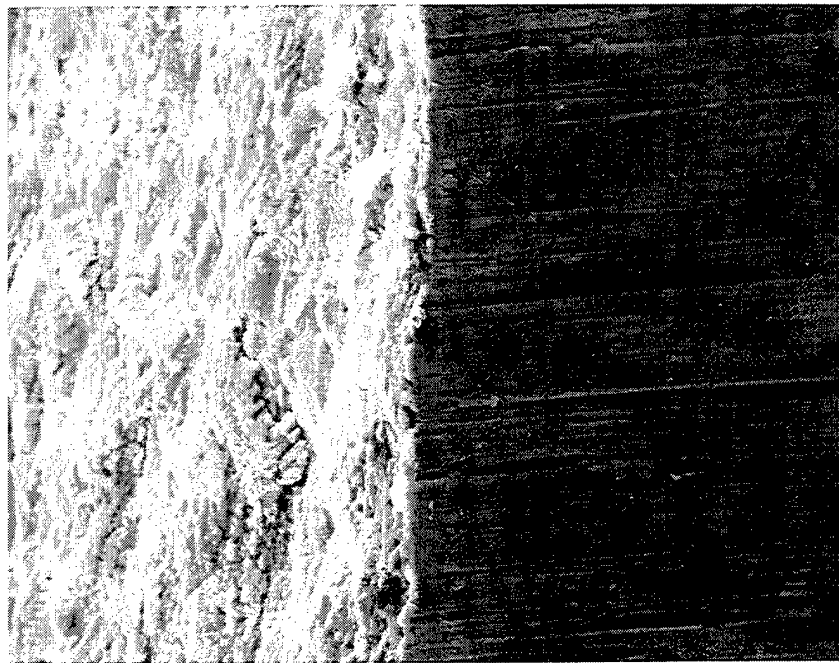


Figure 8. SEM fractograph of SP #6800 10L showing lack of intergranular edge. Mag. 1000 \times .



Figure 9. SEM fractograph of Trial R12 showing an edge origin. Mag. 250×

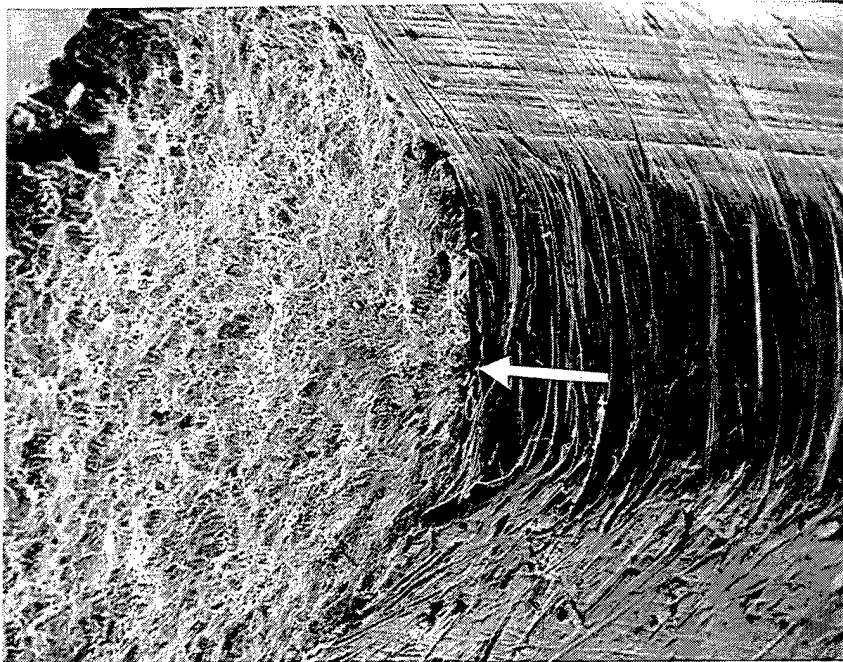


Figure 10. SEM fractograph of Trial R12 showing edge scratches. Mag. 250×

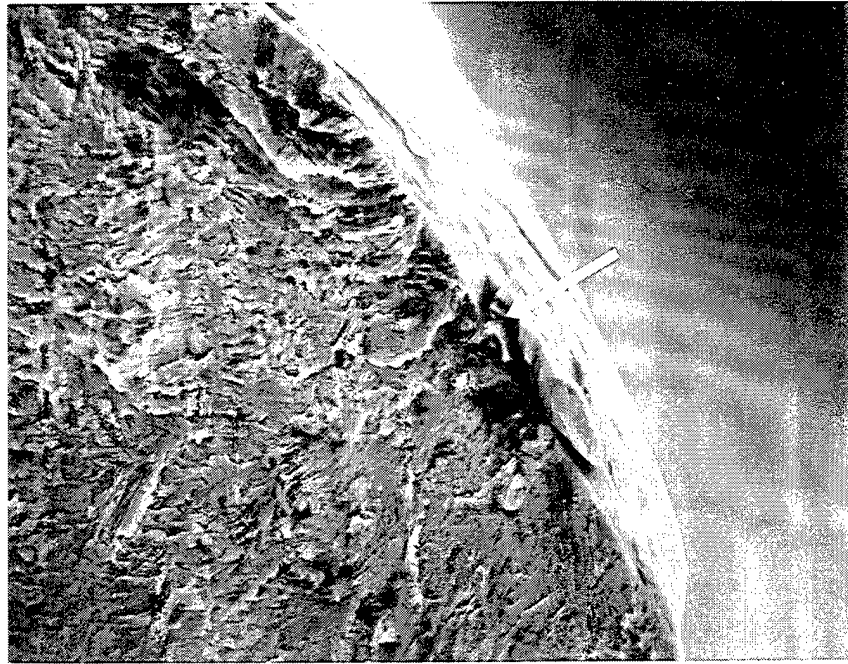


Figure 11. SEM fractograph of Trial R12 showing an edge scratch origin. Mag. 1000x.

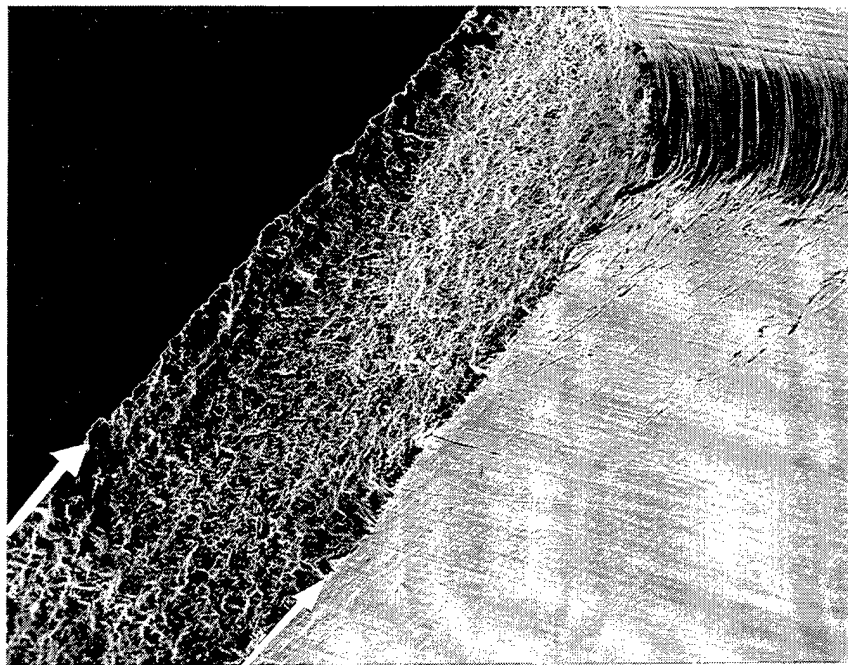


Figure 12. SEM fractograph of Trial R12 showing fatigue by edge intergranular. Mag. 100x.

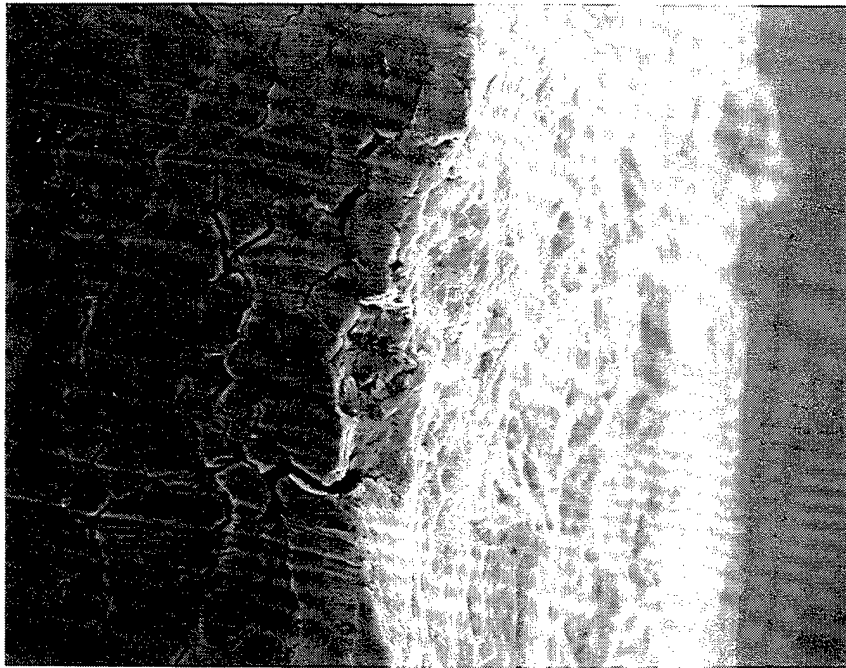


Figure 13. SEM fractograph of Trial R12 showing removed grains on edge. Mag. 750 \times .

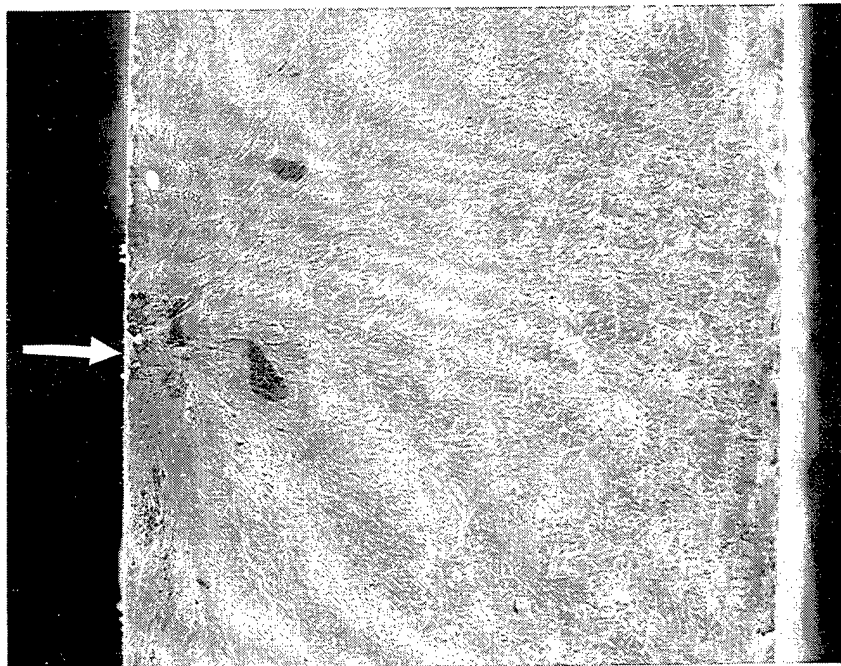


Figure 14. SEM fractograph of low-cost AR showing surface failure origin. Mag. 250 \times .

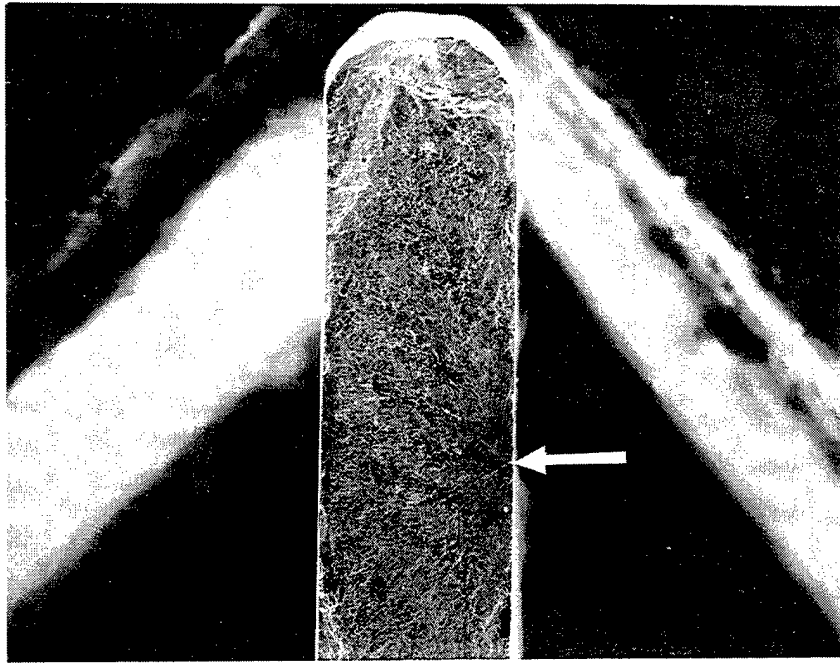


Figure 15. SEM fractograph of low-cost AR showing location of surface origin. Mag. 100x.

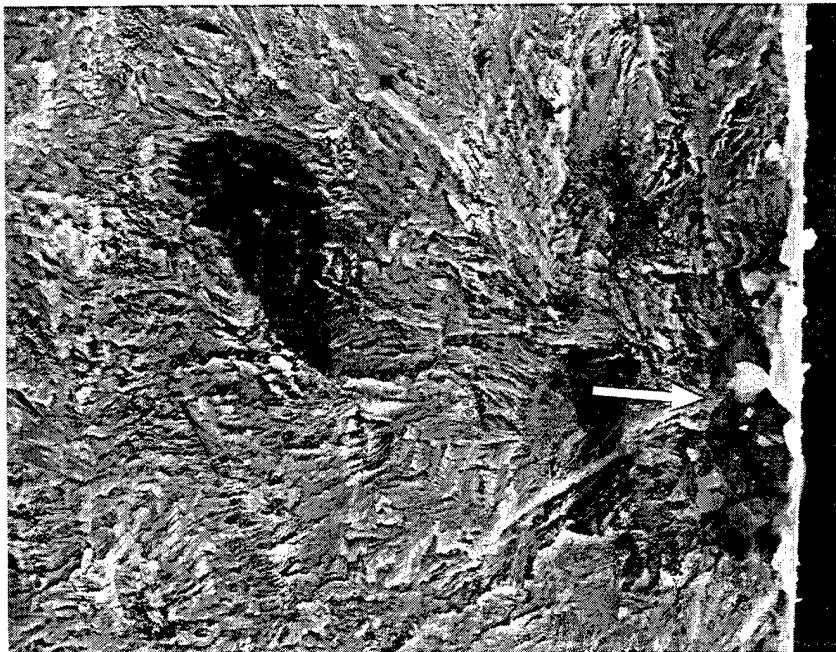


Figure 16. SEM fractograph of low-cost AR showing intergranular at origin. Mag. 1000x.

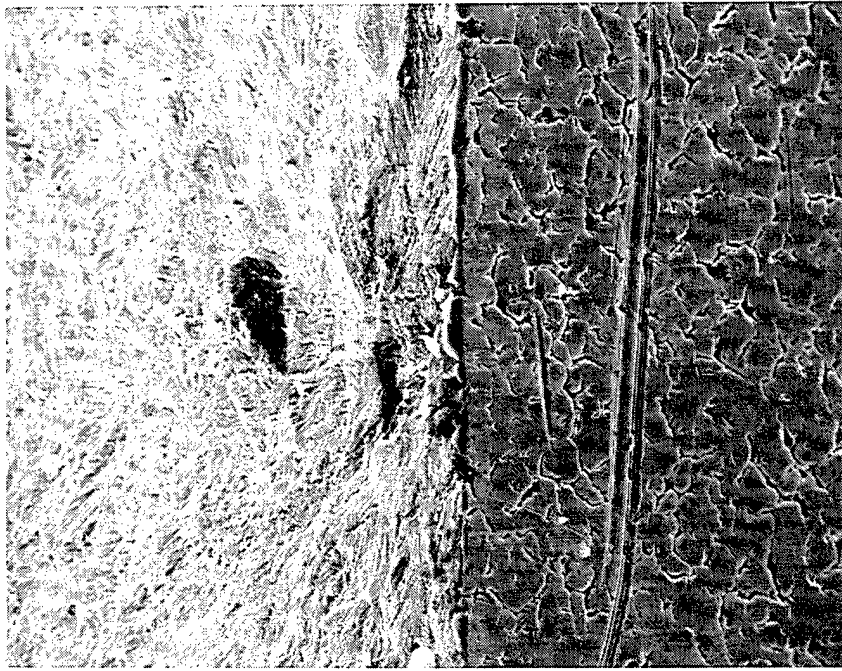


Figure 17. SEM fractograph of low-cost AR intergranular attack near the origin. Mag. 500 \times .

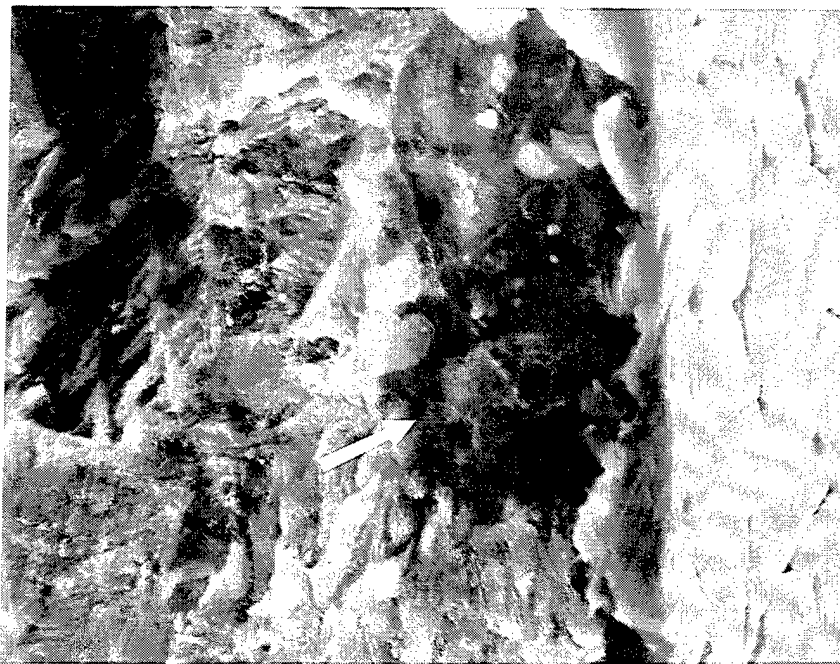


Figure 18. SEM fractograph of low-cost AR intergranular morphology at origin. Mag. 3000 \times .

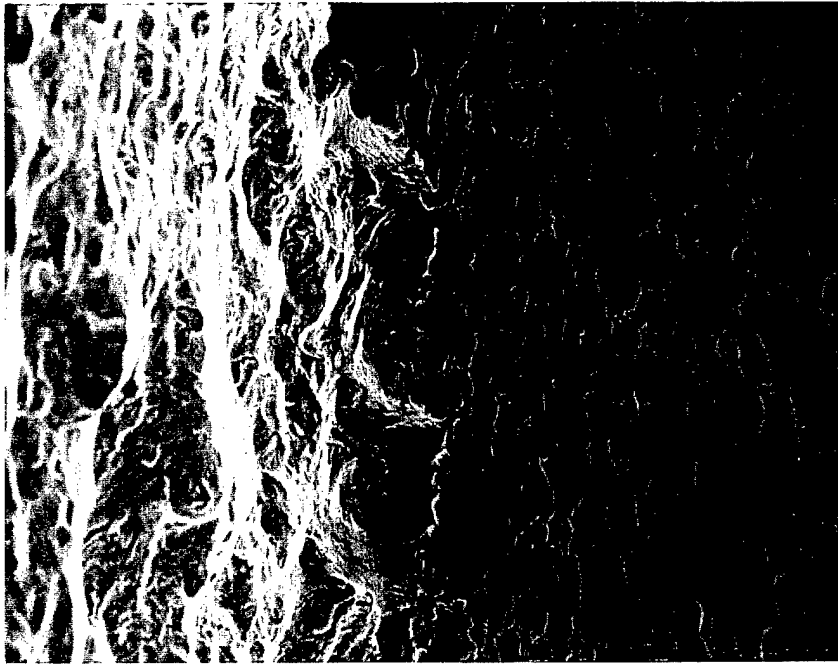


Figure 19. SEM fractograph of low-cost AR removed edge grains and secondary cracking origin. Mag. 500x.

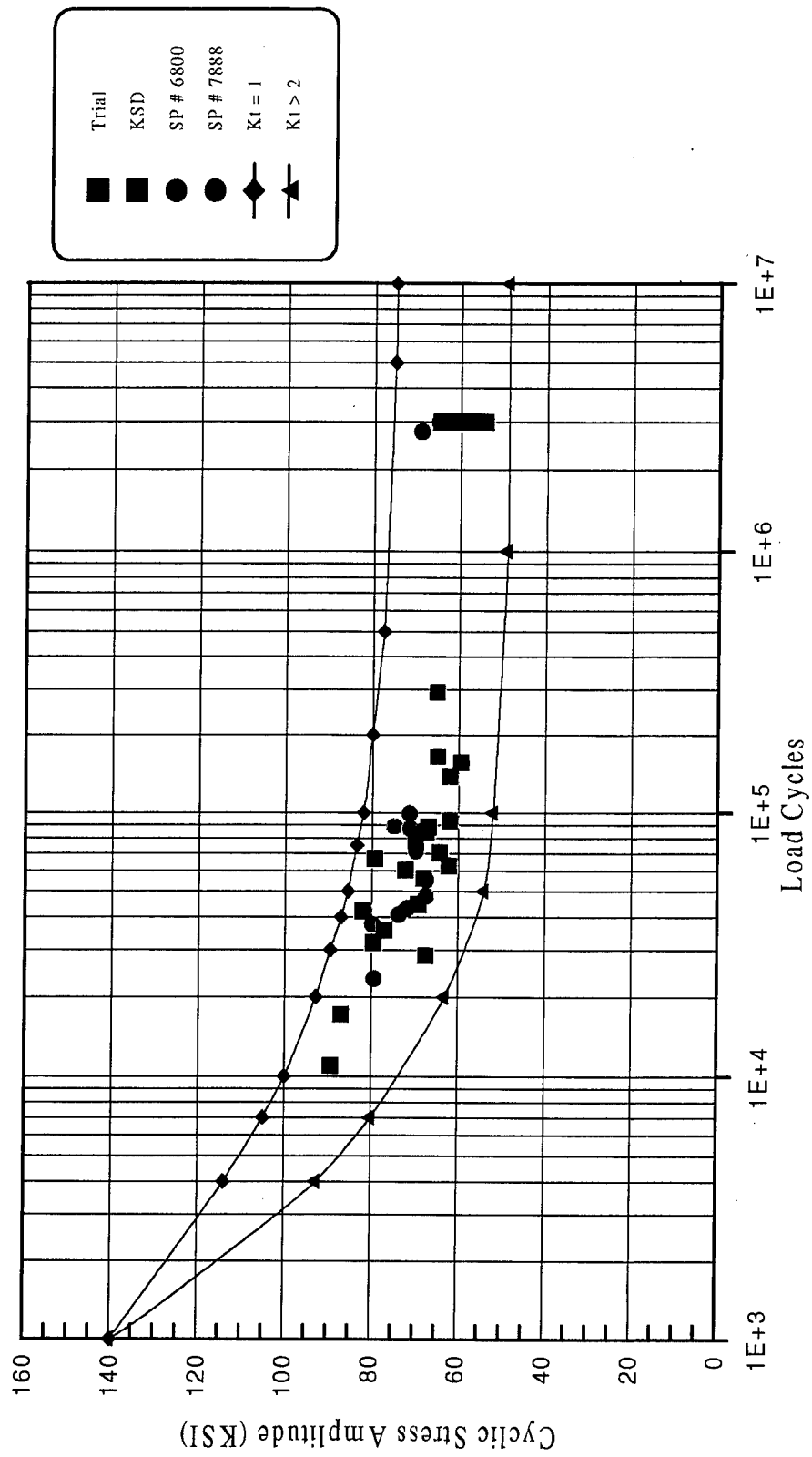


Figure 20. AM355 axial fatigue test - S-N curve; $K_t = 1$; $T = 0.014$; $G = 0.660$; $R = 0.05$.

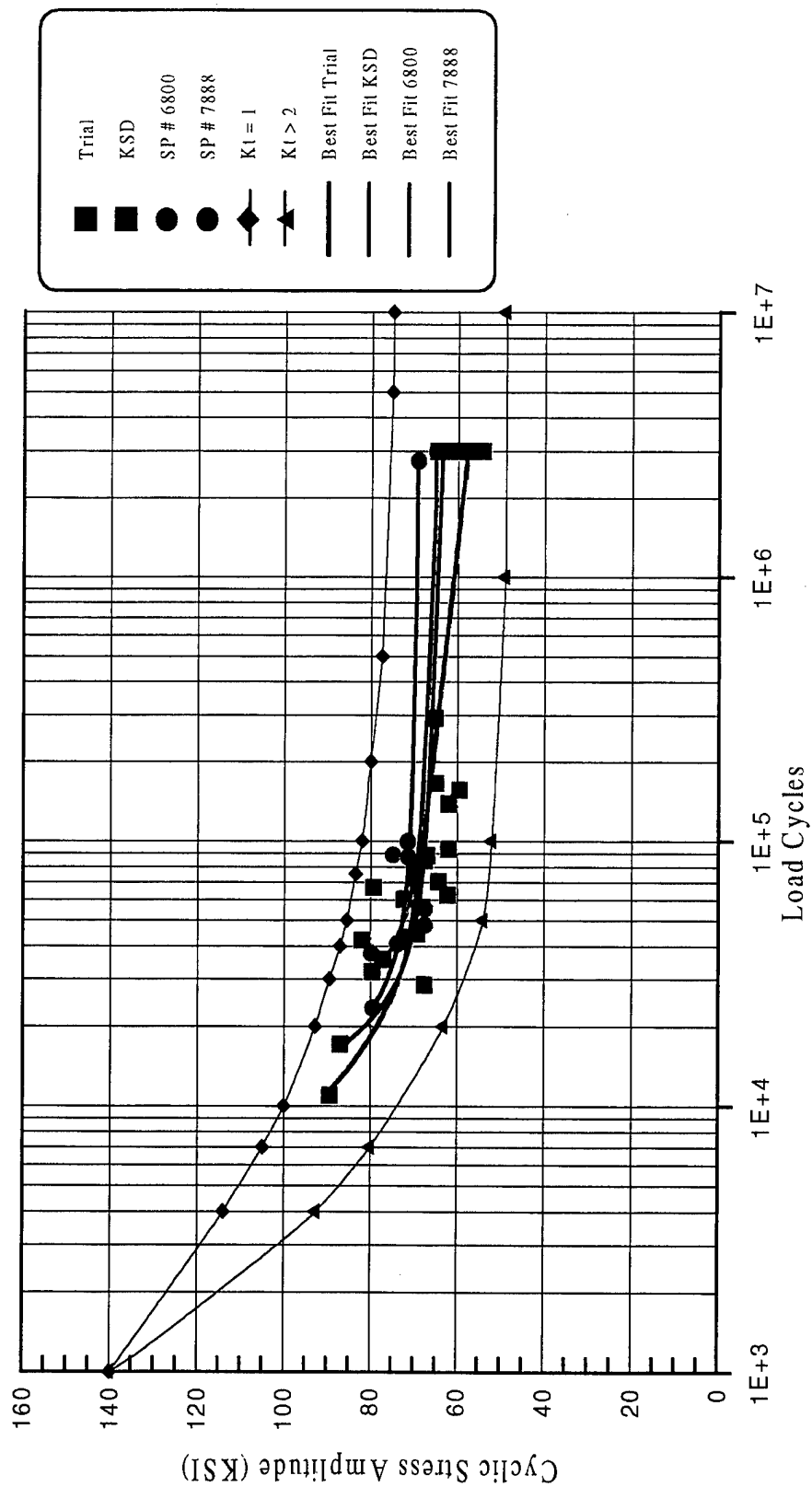


Figure 21. AM355 axial fatigue test - S-N curve; $K_t = 1$; $T = 0.014$; $G = 0.660$; $R = 0.05$; best-fit curves.

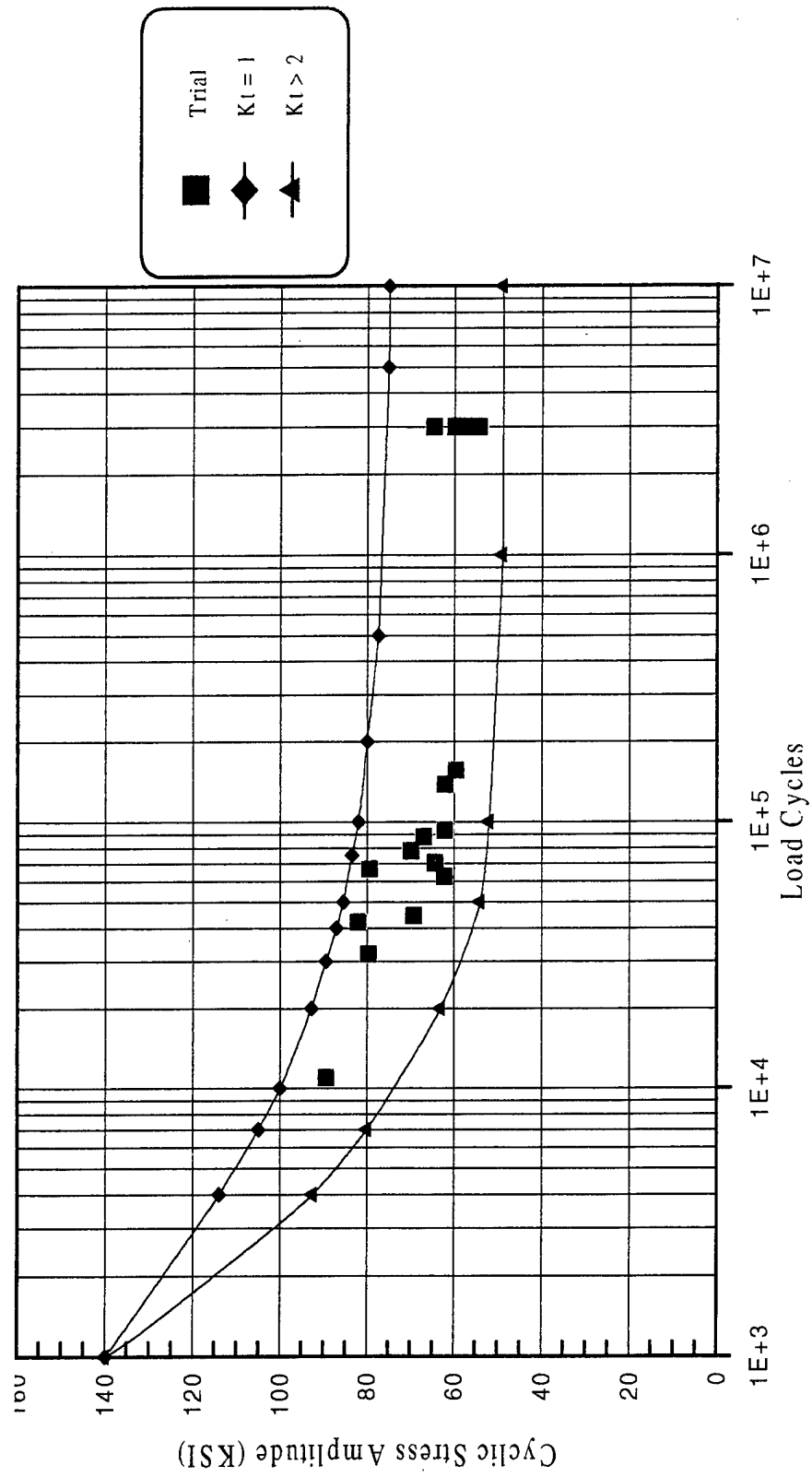


Figure 22. AM355 axial fatigue test - S-N curve; $K_t = 1$; $T = 0.014$; $G = 0.660$; $R = 0.05$; trial.

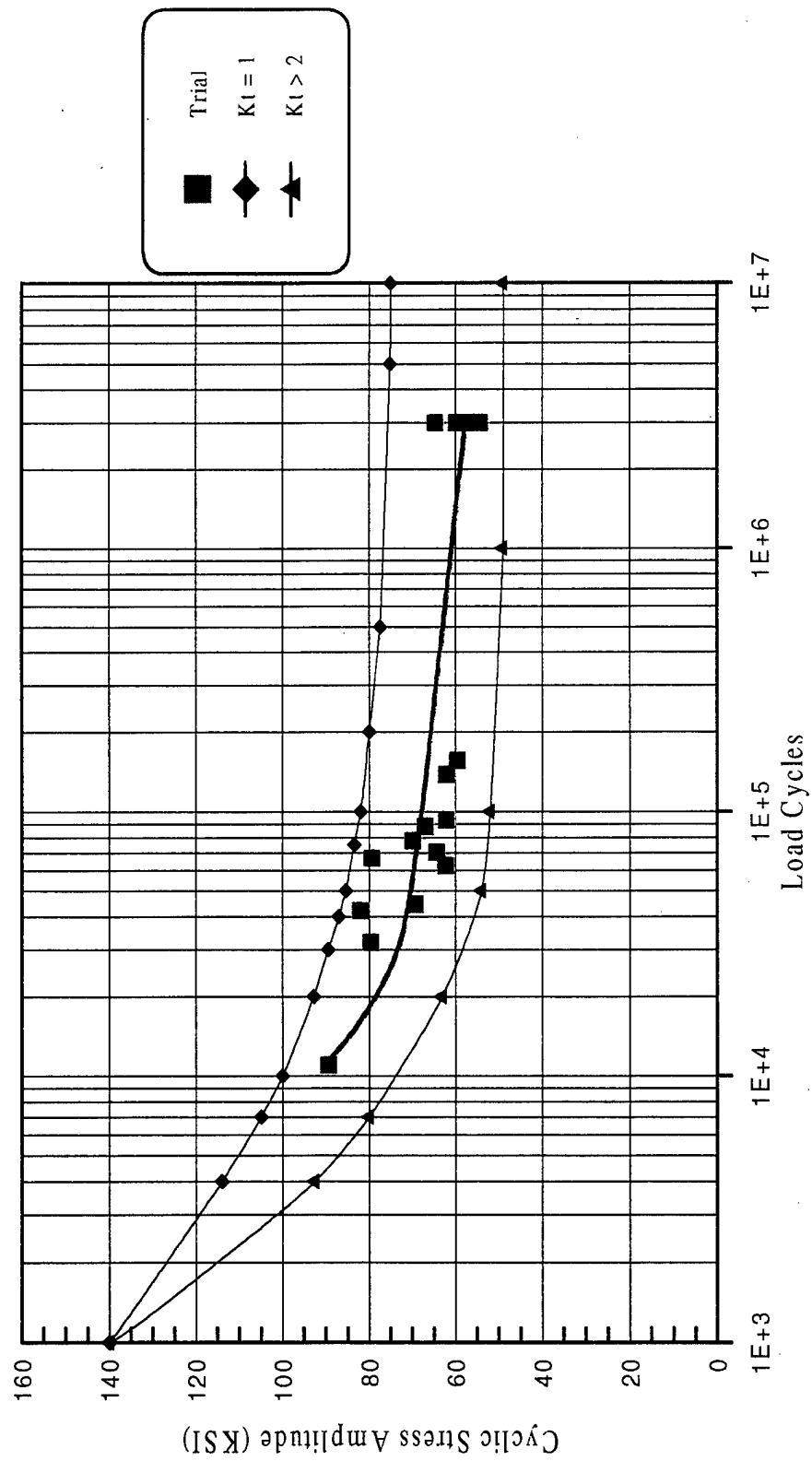


Figure 23. AM355 axial fatigue test - S-N curve; $K_t = 1$; $T = 0.014$; $G = 0.660$; $R = 0.05$; trial best fit.

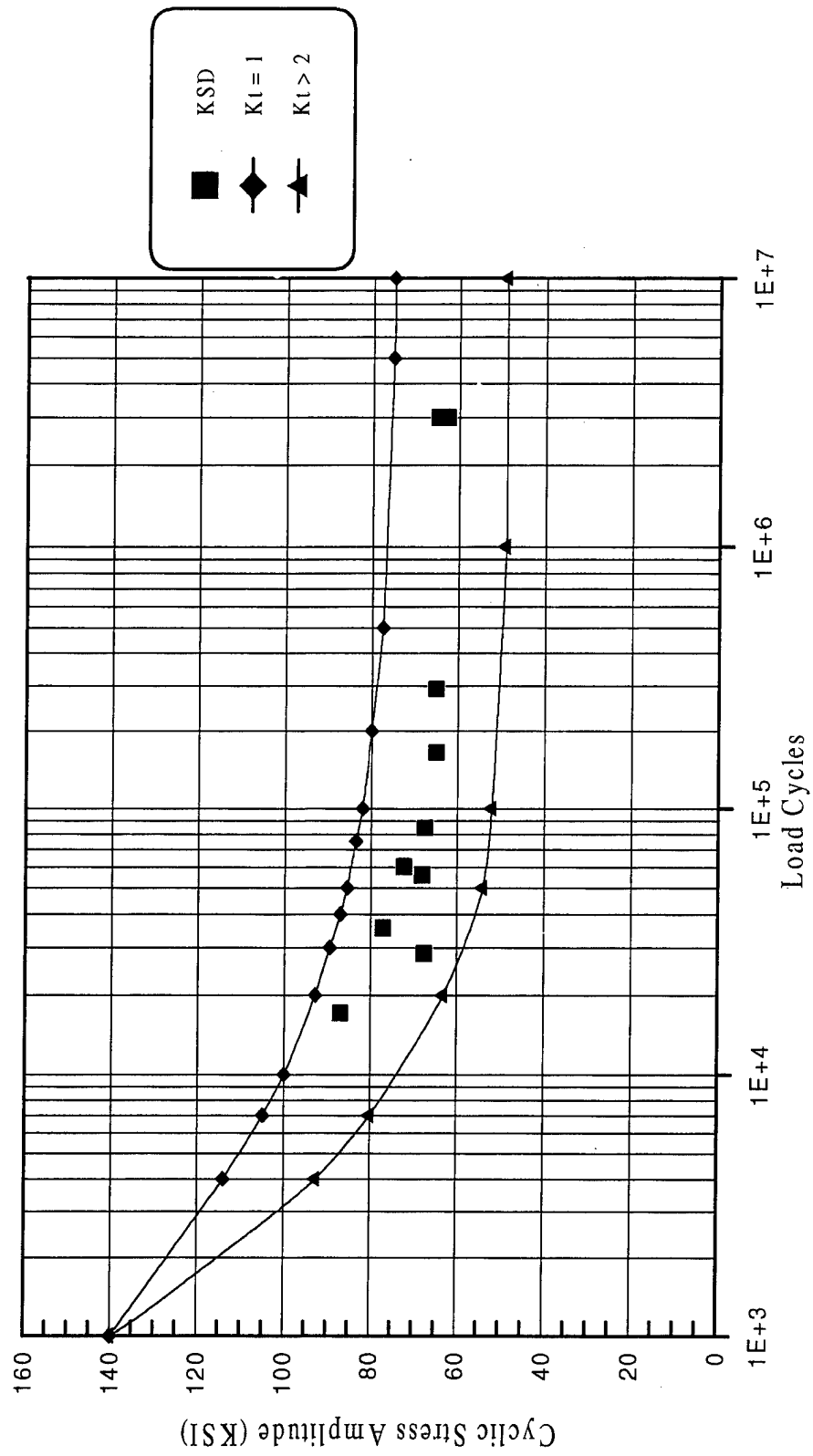


Figure 24. AM355 axial fatigue test - S-N curve; $K_t = 1$; $T = 0.014$; $G = 0.660$; $R = 0.05$; KSD.

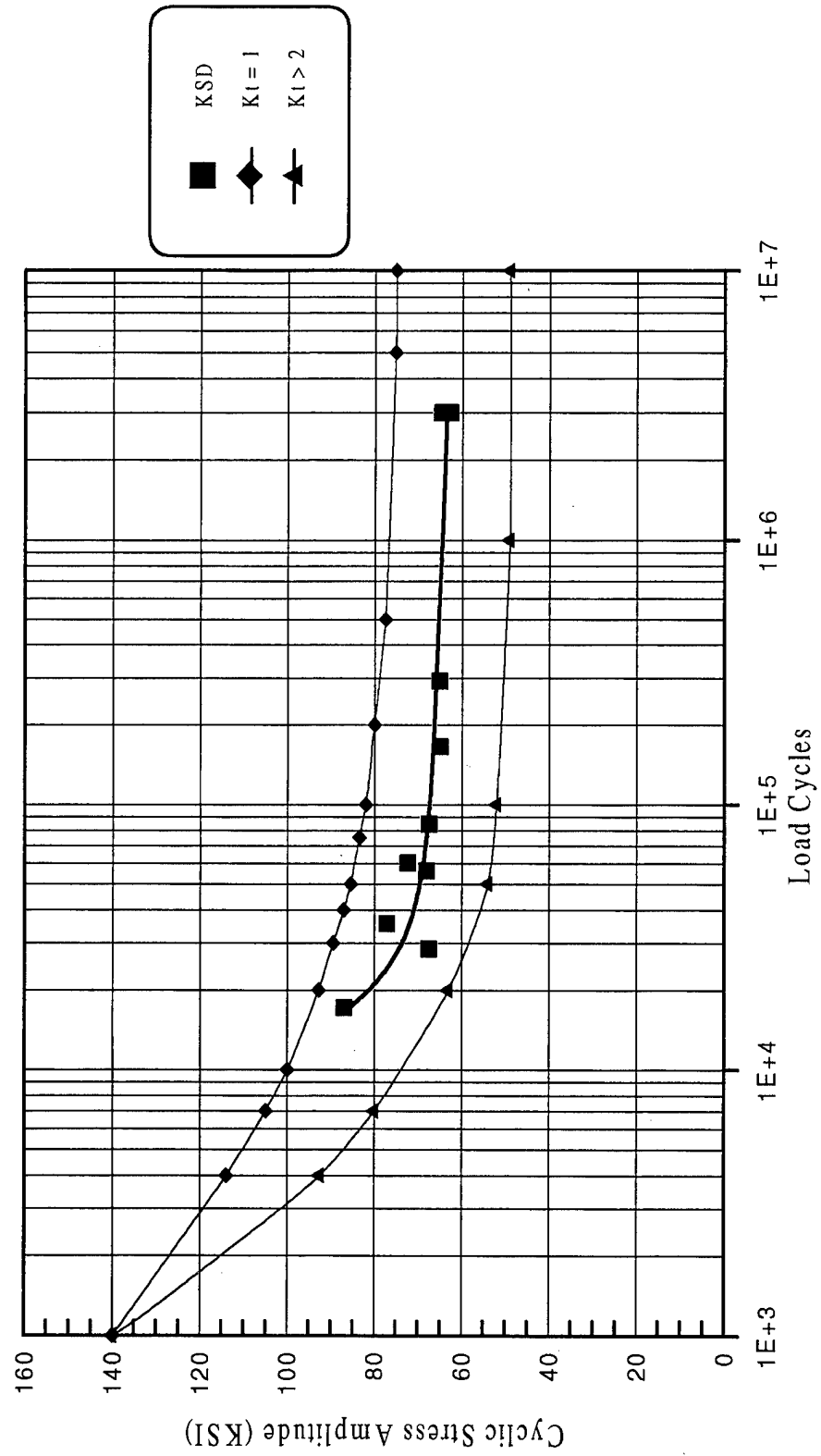


Figure 25. AM355 axial fatigue test - S-N curve; $K_t = 1$; $T = 0.014$; $G = 0.660$; $R = 0.05$; KSD best fit.

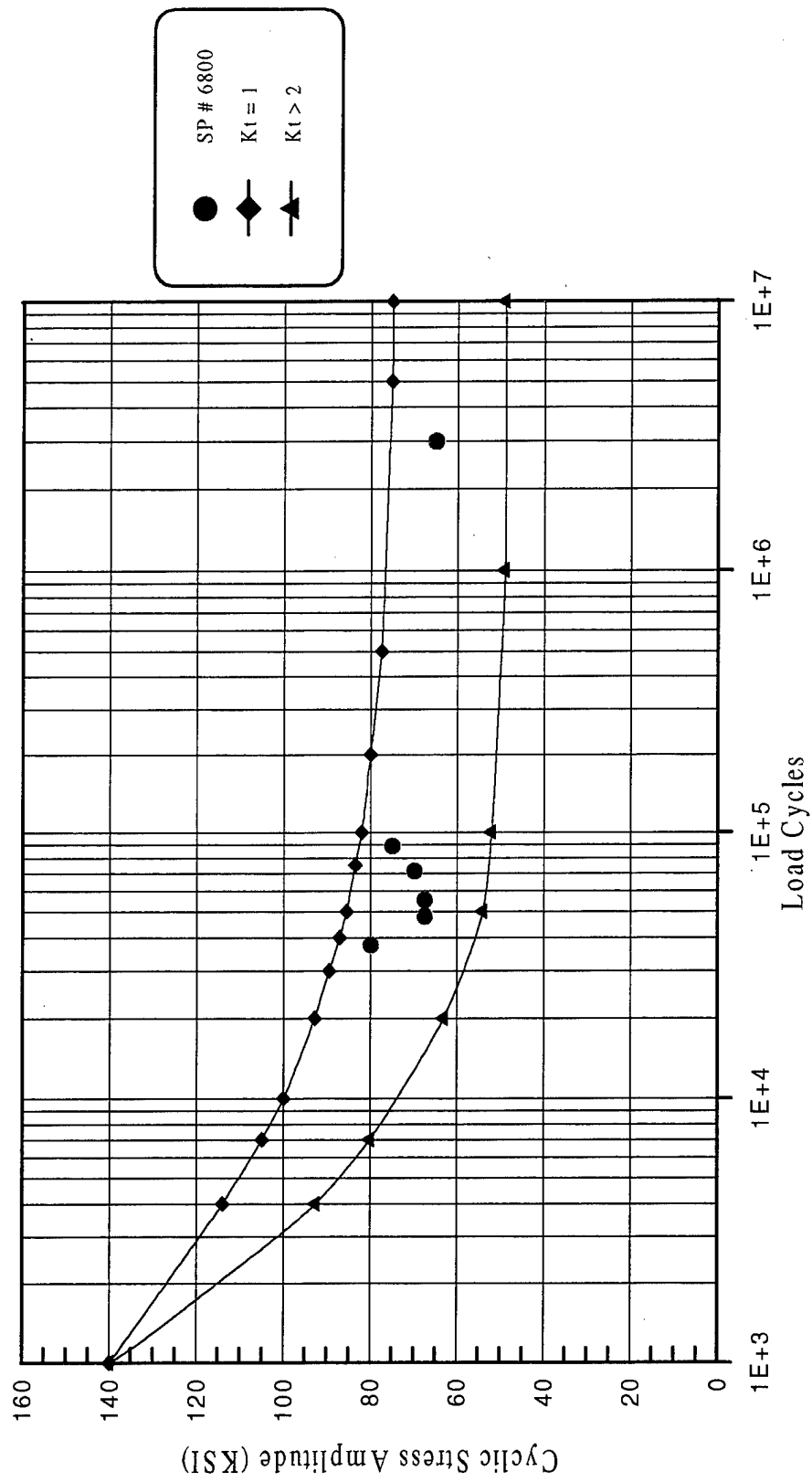


Figure 26. AM355 axial fatigue test - S-N curve; $K_t = 1$; $T = 0.014$; $G = 0.660$; $R = 0.05$; SP #6800.

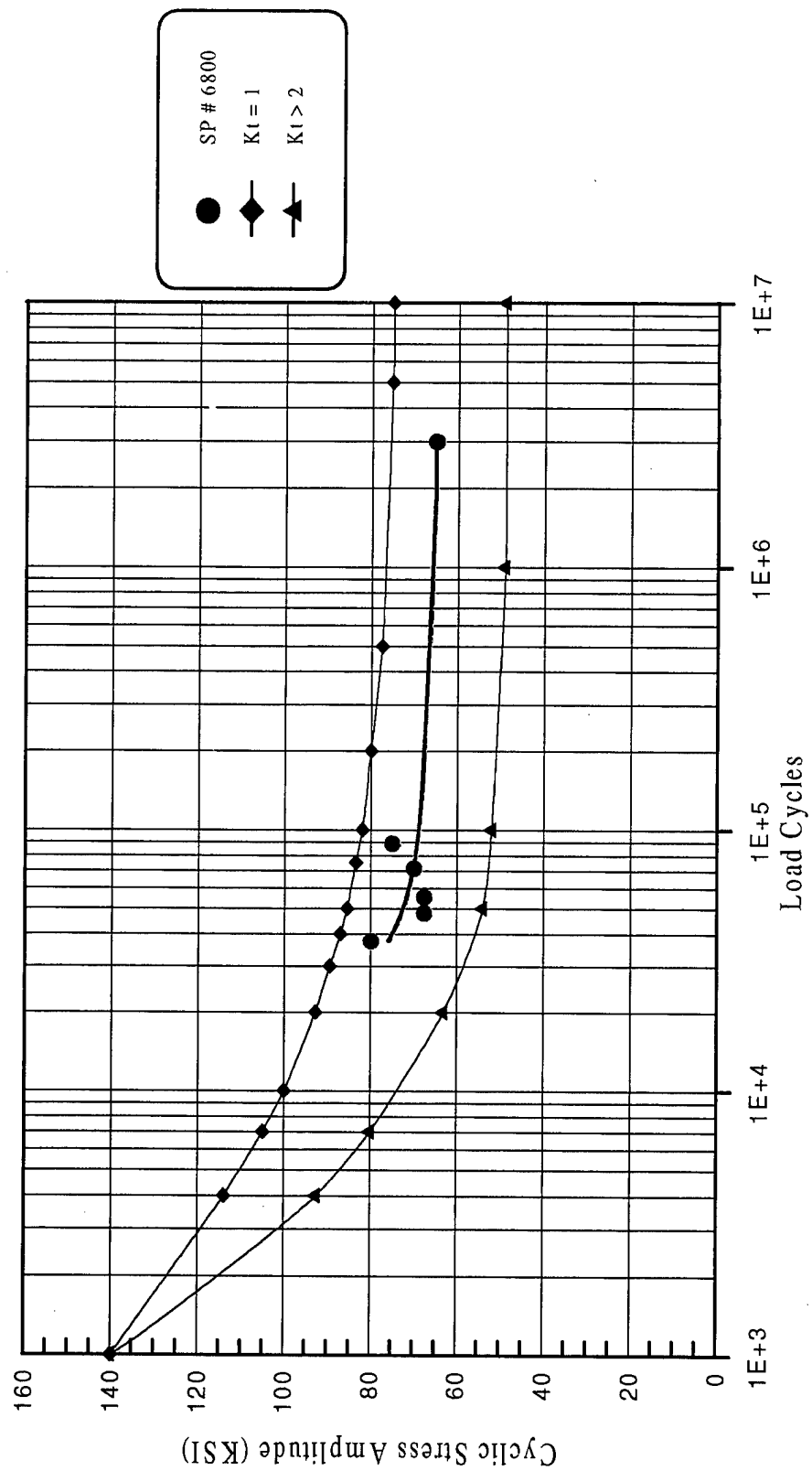


Figure 27. AM355 axial fatigue test - S-N curve; $K_t = 1$; $T = 0.014$; $G = 0.660$; $R = 0.05$; SP #6800 best fit.

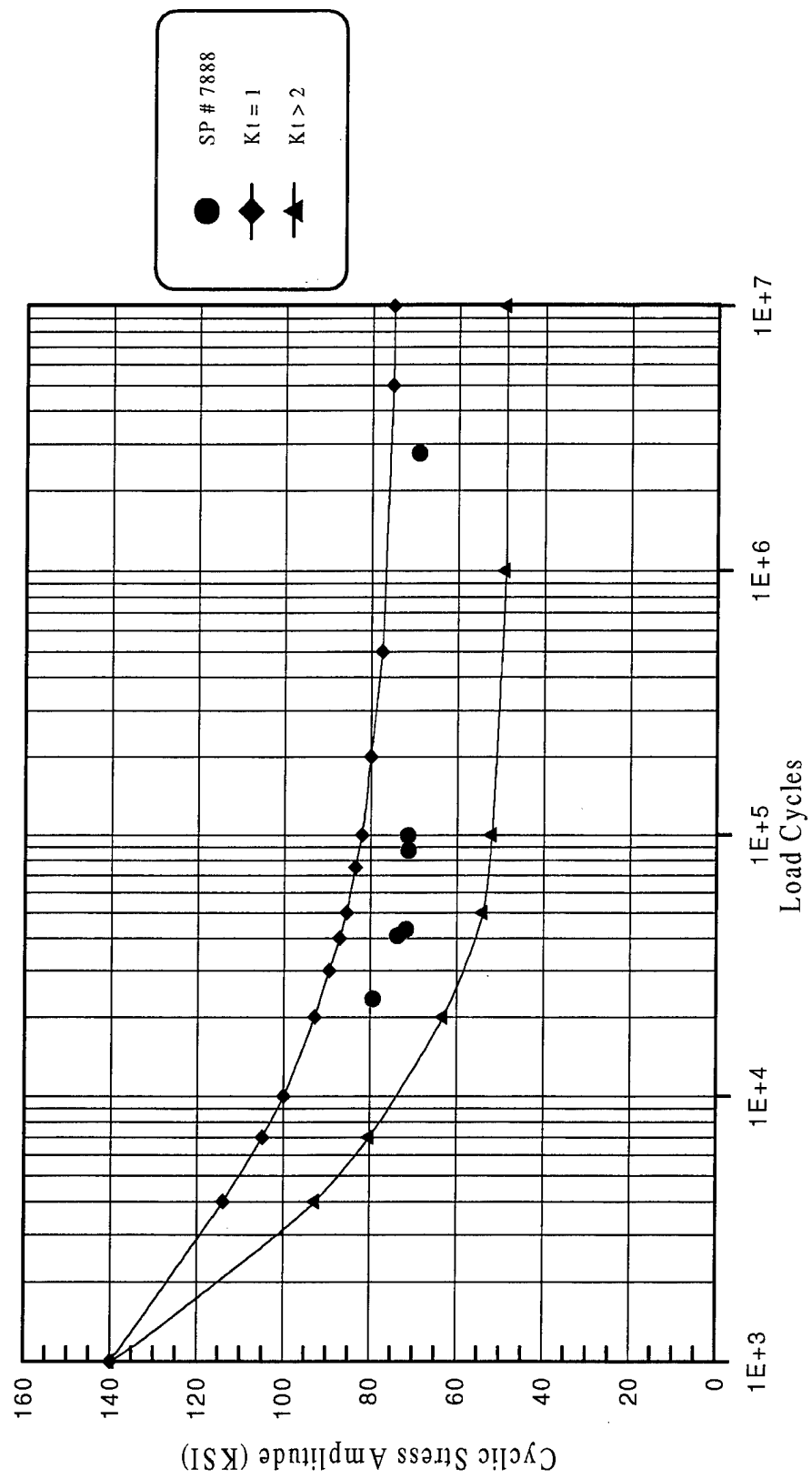


Figure 28. AM355 axial fatigue test - S-N curve; $K_t = 1$; $T = 0.014$; $G = 0.660$; $R = 0.05$; SP #7888.

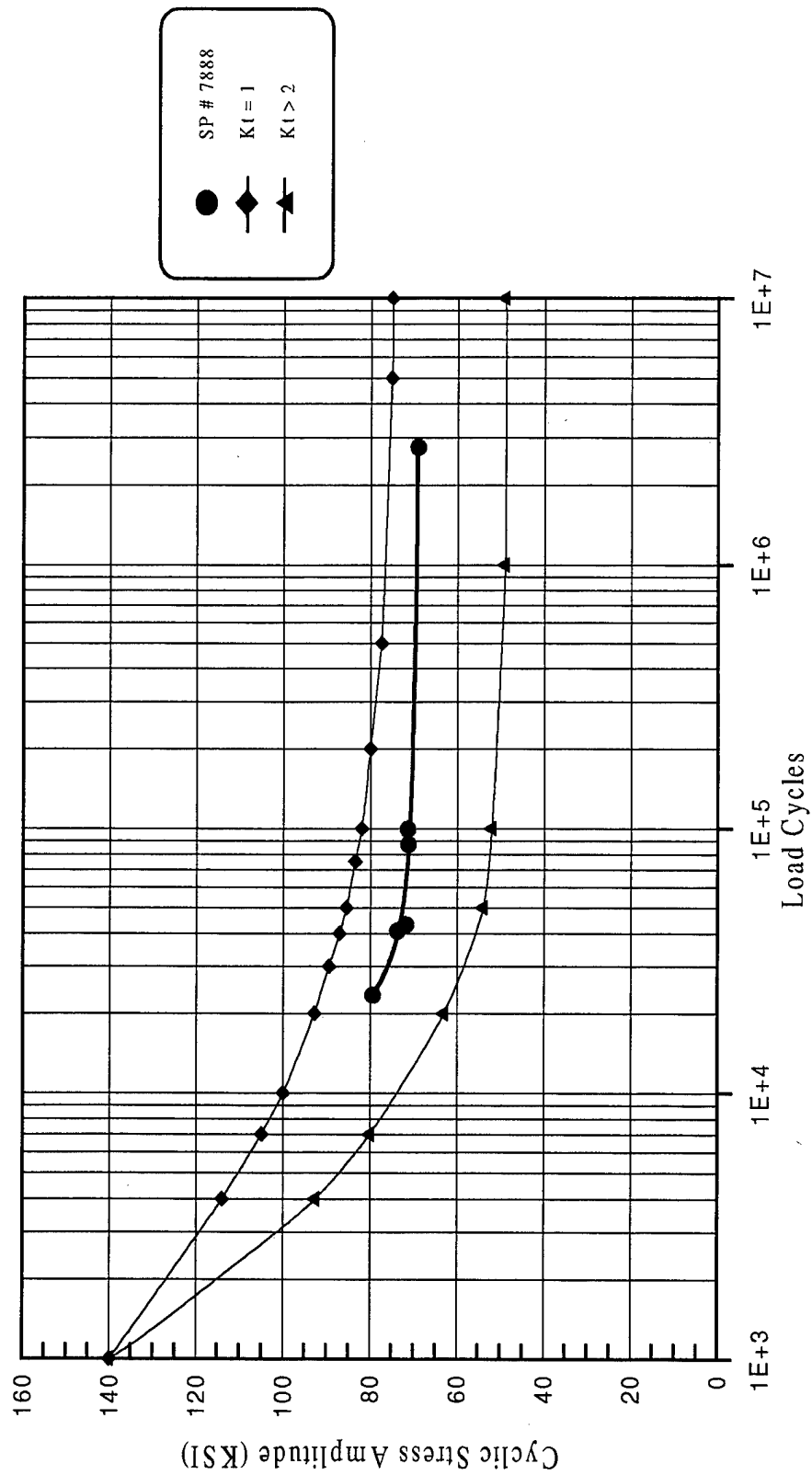


Figure 29. AM355 axial fatigue test - S-N curve: $K_t = 1$; $T = 0.014$; $G = 0.660$; $R = 0.05$; SP #7888 best fit.

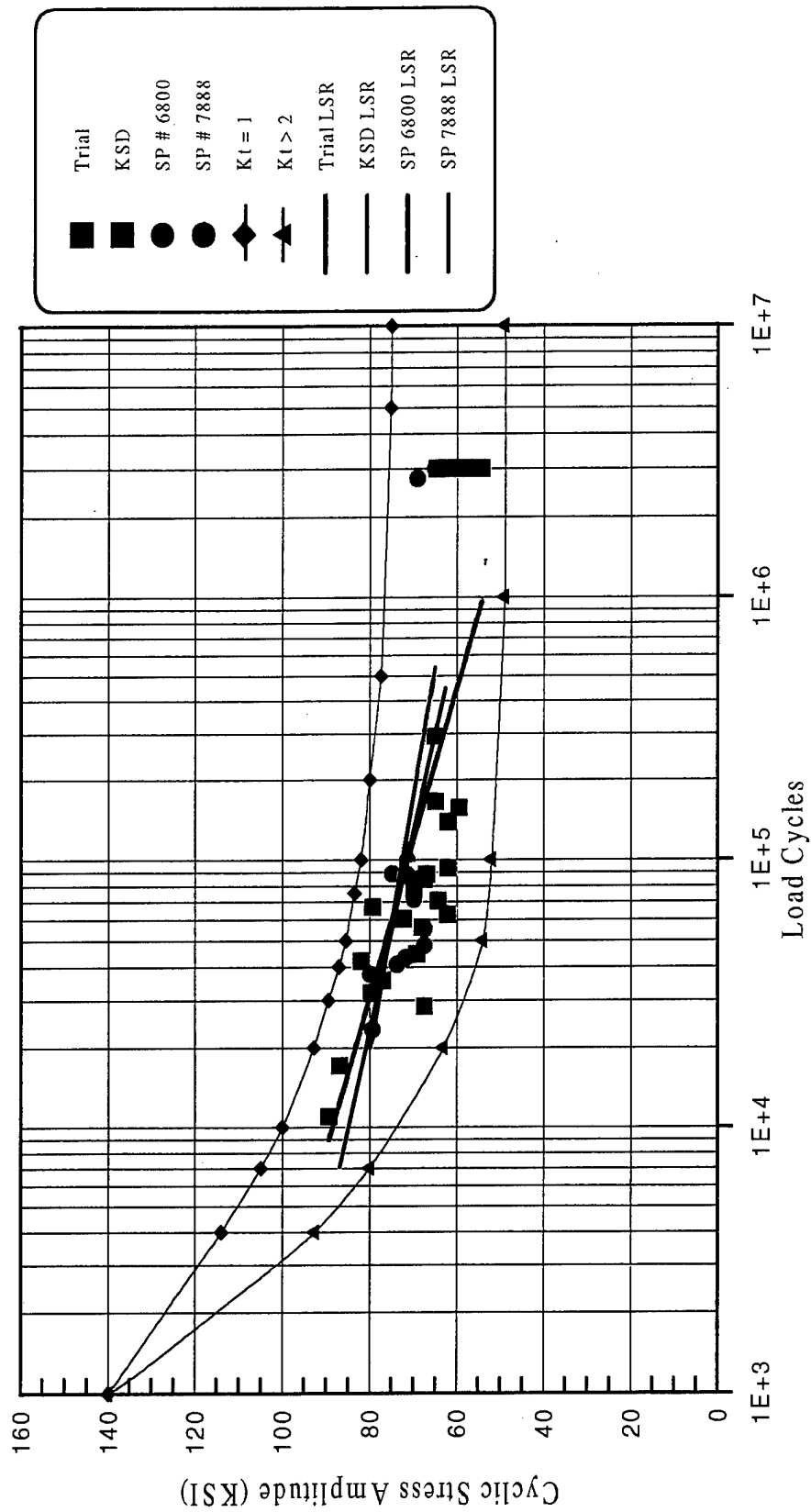


Figure 30. AM355 axial fatigue test - S-N curve; $K_t = 1$; $T = 0.014$; $G = 0.660$; $R = 0.05$; least-squares regression fit.

Least Squares Regression Fit

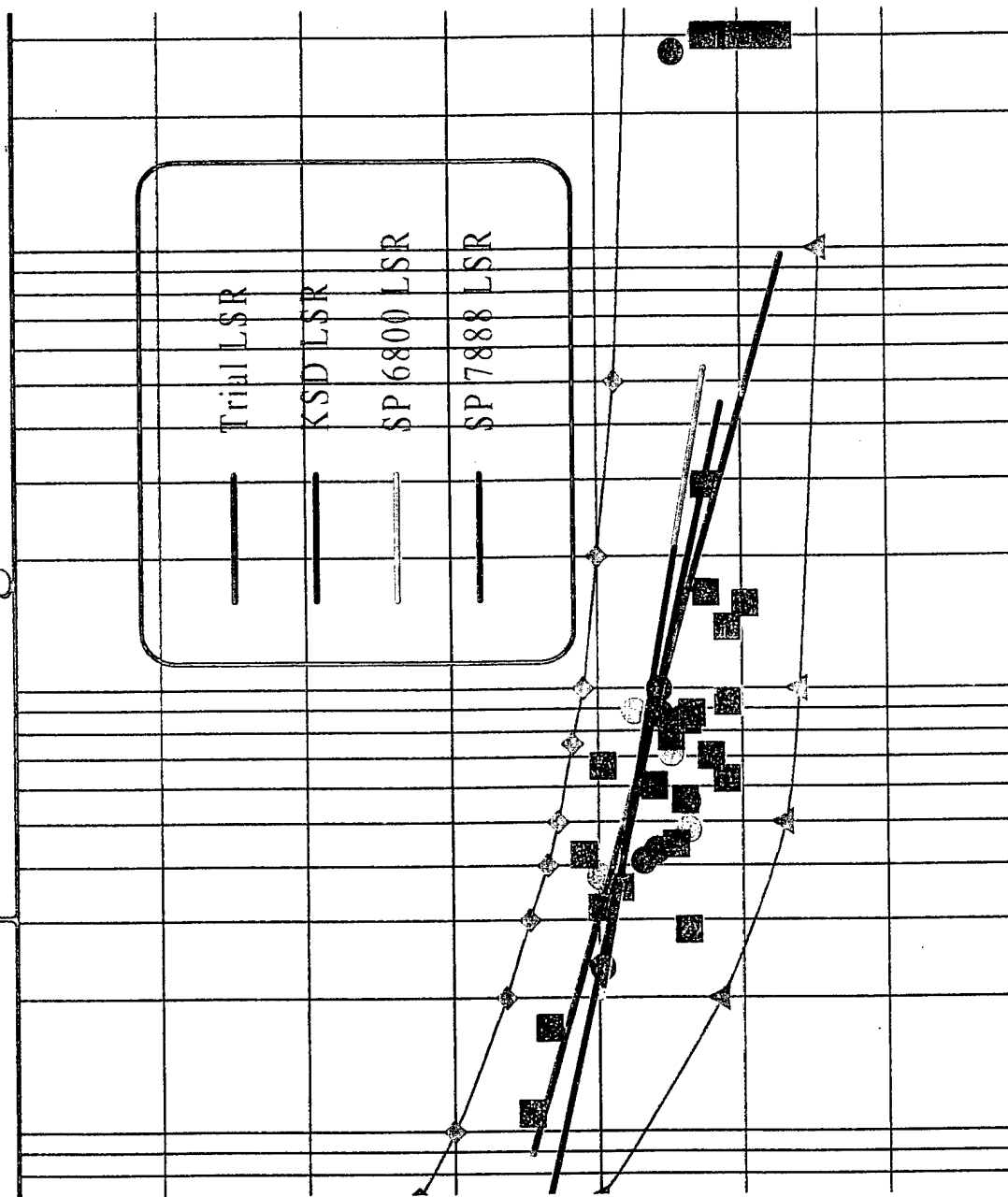


Figure 31. Least-squares regression fit.

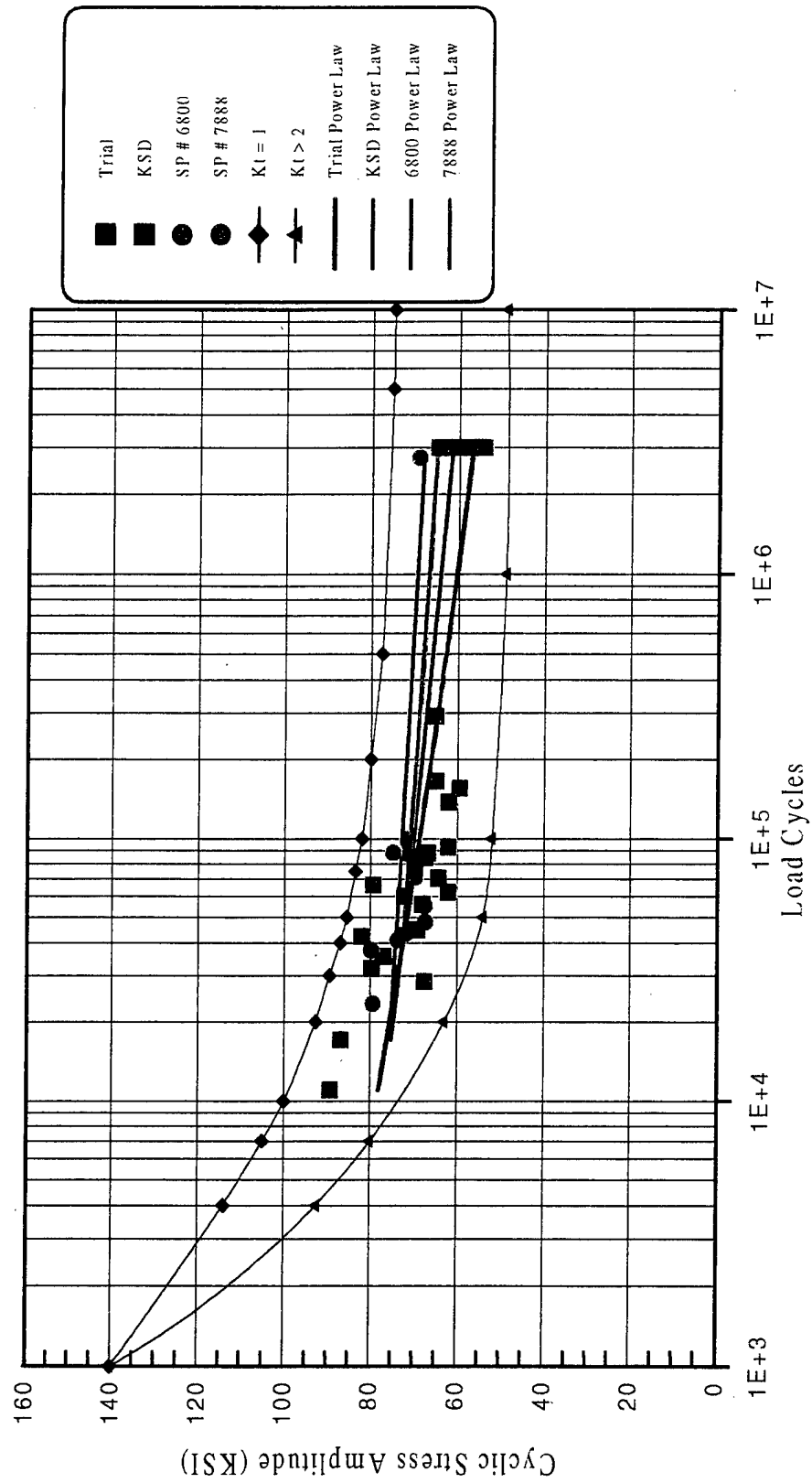


Figure 32. AM355 axial fatigue test - S-N curve: $K_t = 1$; $T = 0.014$; $G = 0.660$; $R = 0.05$; power law fit.

Power Law Fit

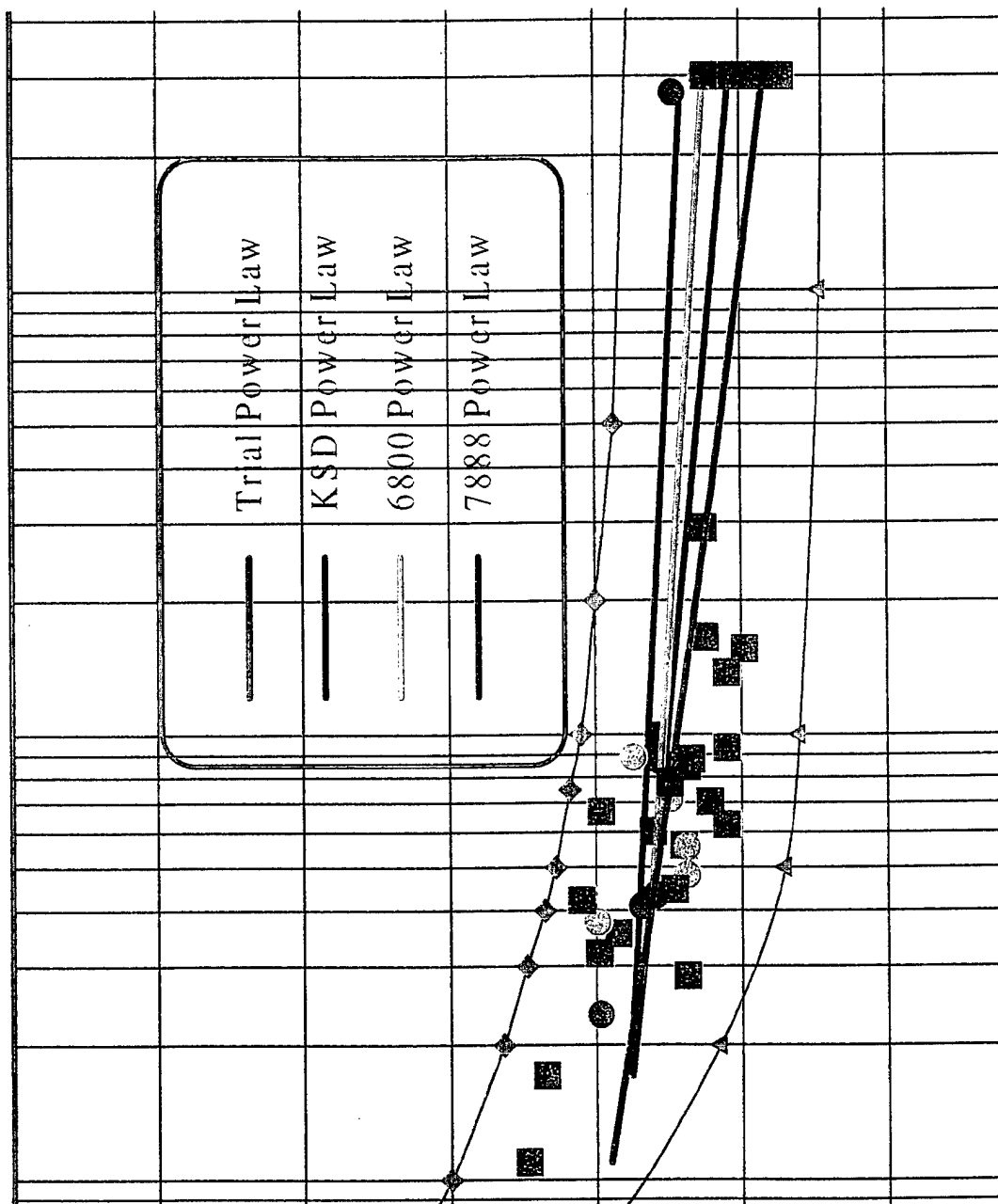


Figure 33. Power law fit.

INTENTIONALLY LEFT BLANK.

<u>NO. OF COPIES</u>	<u>ORGANIZATION</u>
2	DEFENSE TECHNICAL INFO CTR ATTN DTIC DDA 8725 JOHN J KINGMAN RD STE 0944 FT BELVOIR VA 22060-6218

1	DIRECTOR US ARMY RESEARCH LAB ATTN AMSRL CS AL TP 2800 POWDER MILL RD ADELPHI MD 20783-1145
---	---------------------------------------------------------------------------------------------------------

1	DIRECTOR US ARMY RESEARCH LAB ATTN AMSRL CS AL TA 2800 POWDER MILL RD ADELPHI MD 20783-1145
---	---------------------------------------------------------------------------------------------------------

3	DIRECTOR US ARMY RESEARCH LAB ATTN AMSRL CI LL 2800 POWDER MILL RD ADELPHI MD 20783-1145
---	------------------------------------------------------------------------------------------------------

ABERDEEN PROVING GROUND

2	DIR USARL ATTN AMSRL CI LP (305)
---	-------------------------------------

NO. OF
COPIES

ORGANIZATION

2 DIRECTOR
US ARMY AVIATION &
TROOP COMMAND
ATTN AMSAT R EFM
DR KIRIT BHANSALI
4300 GOODFELLOW BLVD
ST LOUIS MO 63120-1798

ABERDEEN PROVING GROUND

2 DIR USARL
ATTN AMSRL MA CB
S GREND AHL
V CHAMPAGNE

USER EVALUATION SHEET/CHANGE OF ADDRESS

This Laboratory undertakes a continuing effort to improve the quality of the reports it publishes. Your comments/answers to the items/questions below will aid us in our efforts.

1. ARL Report Number/Author ARL-TR-1238 (Grendahl) Date of Report November 1996

2. Date Report Received _____

3. Does this report satisfy a need? (Comment on purpose, related project, or other area of interest for which the report will be used.) _____

4. Specifically, how is the report being used? (Information source, design data, procedure, source of ideas, etc.) _____

5. Has the information in this report led to any quantitative savings as far as man-hours or dollars saved, operating costs avoided, or efficiencies achieved, etc? If so, please elaborate. _____

6. General Comments. What do you think should be changed to improve future reports? (Indicate changes to organization, technical content, format, etc.) _____

CURRENT
ADDRESS

Organization

Name

Street or P.O. Box No.

City, State, Zip Code

7. If indicating a Change of Address or Address Correction, please provide the Current or Correct address above and the Old or Incorrect address below.

OLD
ADDRESS

Organization

Name

Street or P.O. Box No.

City, State, Zip Code

(Remove this sheet, fold as indicated, tape closed, and mail.)

(DO NOT STAPLE)

DEPARTMENT OF THE ARMY

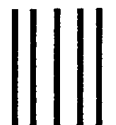
OFFICIAL BUSINESS

BUSINESS REPLY MAIL

FIRST CLASS PERMIT NO 0001,APG,MD

POSTAGE WILL BE PAID BY ADDRESSEE

DIRECTOR
U.S. ARMY RESEARCH LABORATORY
ATTN: AMSRL-MA-C
ABERDEEN PROVING GROUND, MD 21005-5069



NO POSTAGE
NECESSARY
IF MAILED
IN THE
UNITED STATES

